

Factors Affecting the Heat Resistance of *Clostridium perfringens* Spores

Benjamin Carl Orsburn

Dissertation submitted to the faculty of the Virginia Polytechnic Institute and State University in partial fulfillment of the requirements for the degree of

Doctor of Philosophy
In
Biological Sciences

David L. Popham, Chair
Steven B. Melville
Iuliana M. Lazar
Jiann Shin Chen

May 4, 2009

Blacksburg, VA

Keywords: *Clostridium perfringens*, sporulation, heat resistance, food poisoning

Copyright 2009, Benjamin C. Orsburn

Factors Affecting the Heat Resistance of *Clostridium perfringens* spores

Benjamin Carl Orsburn

ABSTRACT

The bacterium *Clostridium perfringens* is a gram-positive anaerobe responsible for many diseases in man and other animals, the most common of which is acute food poisoning (AFP). It is estimated that nearly 240,000 cases of AFP occur each year in the U.S. The *C. perfringens* spore plays an important role in this infection. The heat resistance of the spore allows the organism to survive the cooking process, grow in the cooling food, and infect the victim. Despite the occurrence of this disease and the importance of the spore to this process, little work has been performed to determine how heat resistance is obtained and maintained by *C. perfringens* spores.

In this work we study the spores and sporulation process of *C. perfringens* to determine what factors are most important in the formation of a heat resistant spore. We analyzed the spores produced by nine wild-type strains, including five heat-resistant food poisoning isolates and four less heat-resistant environmental isolates. We determined that threshold core density and a high ratio of cortex peptidoglycan relative to germ cell wall were necessary components of a highly heat-resistant spore. In order to test these observations, we constructed two mutant strains. The first could not achieve the necessary level of core dehydration and rapidly lysed in solution. The second mutant had a reduced amount of cortex relative to germ cell wall, and suffered a corresponding decrease in heat resistance as compared to our wild-type strains. The mutant strains supported the observations drawn from our wild-type strains.

Dipicolinic acid is a major component of bacterial spores and is necessary for spore heat resistance. The Cluster I clostridia, including *C. perfringens*, lack the known DPA synthase operon, *spoVF*. We developed an *in vitro* assay for detecting DPA synthetase activity and purified the active enzyme from sporulating *C. perfringens* crude extract and identified the proteins with mass spectrometry. These results identified the electron transfer flavoprotein alpha chain (EtfA) as the DPA synthase of *C. perfringens*. Inactivating the *etfA* gene in *C. perfringens* resulted in a strain that could begin, but not complete, the sporulation process and produced dramatically lower amounts of DPA than the wild-type. The purified enzyme was shown to produce DPA *in vitro* and utilized FAD as a preferred cofactor.

The results of this research may lead to future techniques to decrease the occurrence of the diseases caused by *C. perfringens* spores and treatments which may carry over to the diseases caused by similar organisms.

DEDICATION

This work is dedicated to my parents, Kenny and Carla. To my father, for always telling us to go to college so that our road would be easier than his, and for only rewarding me when I brought home an 'A' or 'B'. And to my mother for passing on her motto: 'I don't care what you do, so long as you're happy'. Admittedly, there were times when the application of a more disciplined philosophy may have saved me some trouble, but it was definitely more fun this way.

ACKNOWLEDGEMENTS

First, I would like to thank my advisor, David Popham, for his patience throughout my time in his lab. I don't think there many people who could have dealt with the chaos that seems to circle around me at all times. Dave would calmly say 'start at the beginning' and we would work through my procedure until we found the mistake I had been making for a week or month. He even single-handedly quenched the fires of a short-lived microbiology anarchy without raising his voice once.

I would also like to thank the rest of my committee, Steve, Iulia, and Dr. Chen. I don't think we were supposed to get along as well as we did. While I often spent a lot of time feeling very stupid, our meetings were always constructive, extremely informative and almost fun. I don't think I could have picked a better group of people to help me through this project.

Thank you to everyone in the microbiology group. We got our work done and had a lot of fun doing it. I also have to thank the past and present members of the Popham lab for making it the most enjoyable place I can ever imagine working. I am grateful that I could spend these years working side-by-side with some of the best friends I have ever had.

Lastly, I have to thank the graduate school and the registrar's office. After four years in Blacksburg, I had only positive things to say of Virginia Tech. In my final semester and following my defense, these two organizations worked with both diligence and incompetence to darken my opinion of the university.

TABLE OF CONTENTS

ABSTRACT	ii
DEDICATION	iv
ACKNOWLEDGEMENTS	v
LIST OF FIGURES	ix
LIST OF TABLES	x
CHAPTER 1: Introduction and Review of Literature	1
Spores and sporulation	3
Analysis of peptidoglycan structure	7
Dipicolinic acid	9
Objectives of this work	12
CHAPTER 2: Factors affecting the heat resistance of <i>Clostridium perfringens</i> endospores	14
Abstract	15
Introduction	16
Materials and Methods	19
Bacterial strains	19
Spore preparation and determination of heat resistance parameters	19
Determination of spore water content	20
Electron microscopy measurements of spore cross sections	21
Dipicolinic acid (DPA) and spore solute concentrations	21
Determination of spore cortex structure	22
Results	23
Heat resistance and spore core water content	23
Spore dimensions and core volume	24
Spore solute contents	27
Spore cortex structure	28

Discussion	33
Acknowledgements	40
CHAPTER 3: The SpmA/B and DacF proteins of <i>Clostridium perfringens</i> play important roles in spore heat resistance.	41
Abstract	42
Introduction	43
Methods	45
Bacterial strains	45
Spore preparation and determination of D values	46
Determination of spore density	47
Electron microscopy of spore cross sections	47
Dipicolinic acid (DPA) and spore solute concentrations.	47
Determination of spore peptidoglycan structure	48
Statistical analysis	48
Results and Discussion	49
Identification of <i>dac</i> and <i>spm</i> homologues	49
Heat resistance and spore stability	49
Spore density	51
Spore dimensions and core volume	51
DPA and spore solute concentrations	52
Stability of <i>spmA</i> - <i>spmB</i> spores	54
Analysis of spore cortex structure	54
Acknowledgements	57
CHAPTER 4: EtfA is essential for DPA formation in <i>Clostridium Perfringens</i>	58
Abstract	59
Introduction	60
Results and Discussion	62
Purification of the <i>C. perfringens</i> DPA synthase	62
Peptide sequencing results	63
Inactivation of <i>etfA</i> in <i>C. perfringens</i>	64
DPA production by purified DapA and EtfA	67
Occurrence and function of EtfA	68
Proposed function of EtfA in DPA synthesis	69

Alternative methods for DPA production	70
Methods	72
Synthesis of L-ASA	72
In vitro assay for DPA synthase activity	73
Determination of DPA concentration	73
Enrichment of the DPA synthase from NCTC 8679	74
Native-PAGE assays for DPA synthase activity	74
Construction of mutant strains	75
Purification of DapA and EtfA	76
Acknowledgements	77
CHAPTER 5: Final Discussion	78
REFERENCES	83

LIST OF FIGURES

Chapter 1

- Figure 1.1. Depiction of the sporulation of *B. subtilis*. 4
- Figure 1.2. The main structural characteristics a bacterial spore. 5
- Figure 1.3. Vegetative peptidoglycan structure compared to cortex structure. 7
- Figure 1.4. Simplified overview of the DPA synthesis pathway 10

Chapter 2

- Figure 2.1. TEM images of *C. perfringens* spore cross sections. 26
- Figure 2.2. Heat resistance correlates with the P/S ratio in *C. perfringens*. 27
- Figure 2.3. HPLC separation and MS analysis of *C. perfringens* SM101 spore
muropeptides. 30

Chapter 3

- Figure 3.1. TEM images of *Clostridium perfringens* spore cross-sections. 52

Chapter 4

- Figure 4.1. Mechanism of DPA formation. 61
- Figure 4.2. Scale representation of the locus containing *etfA*. 64
- Figure 4.3. Production of DPA by each strain during sporulation. 65
- Figure 4.4. Phase contrast images of SM101 and *Etf1* during sporulation. 66

LIST OF TABLES

Chapter 2

Table 2.1. <i>C. perfringens</i> spore heat resistance and water content.	24
Table 2.2. <i>C. perfringens</i> spore dimensions and core volumes.	25
Table 2.3. <i>C. perfringens</i> spore solute contents.	28
Table 2.4. Muropeptides produced from <i>C. perfringens</i> spore PG.	31
Table 2.5. Monosaccharide fragment analysis of muropeptide 18.	32
Table 2.6. <i>C. perfringens</i> spore PG structural parameters.	32
Table 2.7. Requirements for establishing a highly heat-resistant spore.	38

Chapter 3

Table 3.1. Primers used in this study (Chapter 3).	45
Table 3.2. Spore heat resistance and wet density.	50
Table 3.3. <i>C. perfringens</i> spore dimensions and core volumes.	52
Table 3.4. <i>C. perfringens</i> spore solute contents.	53
Table 3.5. Biochemical characterization of the PG of <i>C. perfringens</i> spores.	56

Chapter 4

Table 4.1. Purification of the DPA synthase of <i>C. perfringens</i>	63
Table 4.2. Summary of <i>in vitro</i> assays with purified EtfA.	69
Table 4.3. Primers used in this study (Chapter 4).	76
Table 4.4. Strains used in this study (Chapter 4).	76

Chapter 1

Introduction and Review of Literature

Clostridium perfringens is an anaerobic, spore forming bacteria responsible for a number of pathogenic conditions affecting man and other mammals. As early as 1914, this organism was recognized as the most common cause of gas gangrene. Other research occurring during the same time period also associated this organism with outbreaks of mild diarrhea and cramps that we now know to be characteristic of acute food poisoning (AFP). *C. perfringens* strains are classified into five groups, typed A-E, based on the number and combination of toxins produced by the strain. The conditions caused by *C. perfringens* strains are varied, but are often broadly classified into necrotic-type diseases and enterotoxemias (Reviewed in, (23)).

The most common disease produced by this organism is AFP. This condition is caused only by a subgroup of Type A strains that produce the *Clostridium perfringens* enterotoxin, CPE. Although less than five percent of the global *C. perfringens* population is believed to carry the *cpe* gene (51), this toxin is responsible for over 240,000 cases of food poisoning annually in the United States (61). AFP occurs following consumption of large numbers of vegetative bacteria that sporulate in the gastrointestinal tract, simultaneously releasing CPE. Once released, CPE attaches to the villus tip cells of the small intestine, causing a disruption in the ability to maintain membrane ionic balance which results in the characteristic diarrheal symptoms (18). AFP is self-limiting as the massive release of water effectively removes the cells from the digestive tract. Most patients recover in 24-48 hours, with no additional symptoms, leading to the misnomer for this condition, 'the 24 hour flu' (79). Although the risk of Type A food poisoning can be virtually eliminated when proper procedures pertaining to refrigeration and reheating

of food are observed, it continues to be a major problem, primarily in commercial food production (61).

A survey of *C. perfringens* strains in 1985 by Ando *et al.*, noted that strains producing CPE (CPE+) appeared to produce spores with greater relative heat resistance than strains that lacked the toxin (CPE-) (2). Since that initial work a number of studies supported this finding and have demonstrated that CPE+ strains demonstrate superior heat resistance as both vegetative cells and as spores than CPE- strains (64, 81).

Spores and sporulation.

Sporulation is a survival strategy employed by a wide number of Clostridia and Bacilli. These organisms have the ability to form a dormant cell type that is resistant to a large number of environmental stresses that would kill a vegetative cell of the same species. The resistance features of *Bacillus anthracis* spores were observed more than a century ago by Robert Koch when he observed that some cells of the species could survive boiling. Around that same time Ferdinand Kohn was observing the sporulation process of *B. subtilis* by light microscopy. These studies first noted the morphological changes these cells undergo during the sporulation process as well as the increase in resistance properties accompanied by these changes (Reviewed in, (31)).

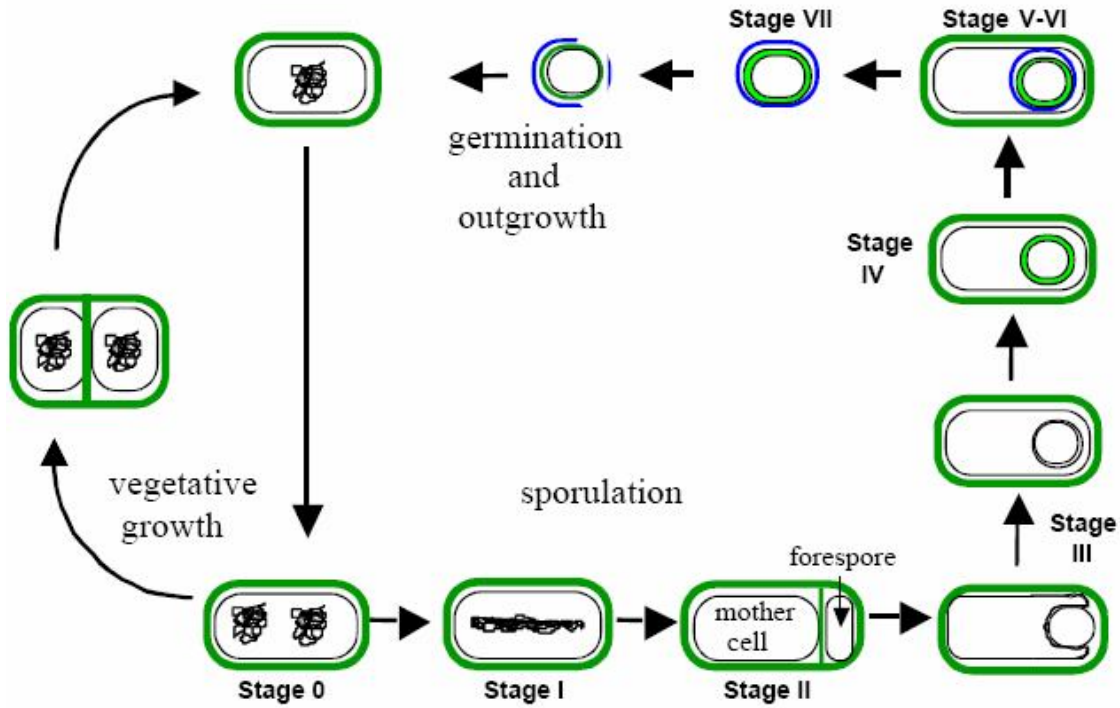


Figure 1.1. Depiction of the sporulation of *B. subtilis*.

The diagram above demonstrates the life cycle of the model sporulating bacteria, *Bacillus subtilis*. Under normal growth conditions, the spore forming bacteria have no reason to continue anything but normal vegetative growth. During nutrient-limiting conditions, however, an entirely new set of global transcription factors become activated that serve to produce the new cell type (35). The morphological changes of *C. perfringens* follow a similar pattern, though genomic analysis has indicated that although most genes are conserved, a number of genes essential for sporulation in *B. subtilis* are not found in *C. perfringens*, such as *spoVF* (66, 72).

Figure 1.2 The main structural characteristics of a bacterial spore.

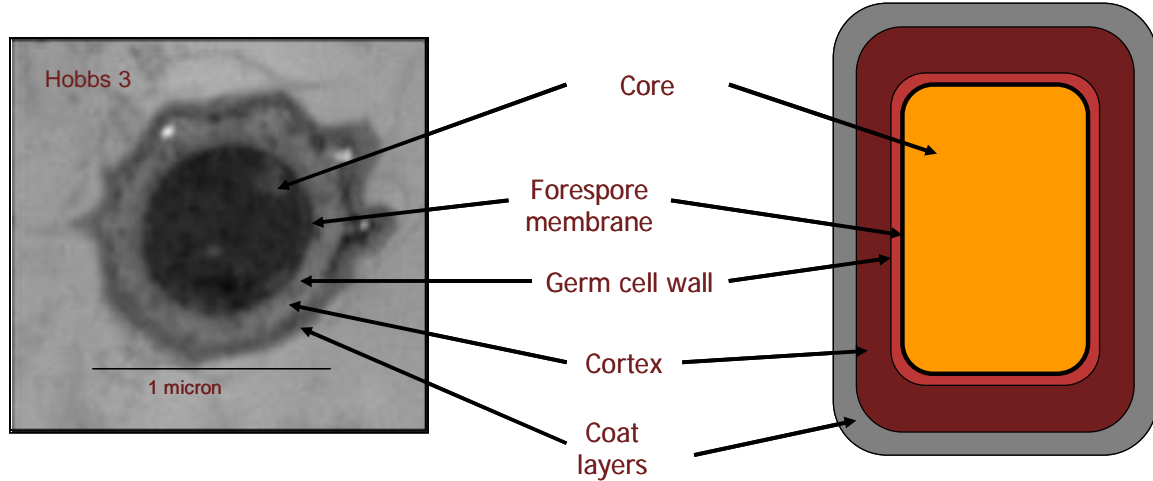


Figure 1.2 is a simplified representation of the components of a bacterial spore. On the left is a sectioned spore from a *C. perfringens* Hobbs serotype 3 strain. In the center of the spore is the core. The core is the equivalent of the cellular cytoplasm, containing the chromosome and essential cellular machinery. Unlike the cytoplasm of a vegetative cell, the spore core is highly dehydrated and filled with a high concentration of small molecules such as dipicolinic acid (DPA) and small acid soluble proteins (SASPs) (86) that serve to protect the chromosome and essential proteins as well as high concentrations of divalent cations such as Ca^{2+} , Fe^{2+} and Mg^{2+} (91). The core is surrounded by the forespore membrane, an impermeable layer that is highly resistant to osmotic stress. A survey of spores formed by different organisms observed that more heat resistant spores generally possessed more dehydrated spore cores (12).

Two layers of peptidoglycan surround the forespore membrane. The inner layer is known as the germ cell wall, which is essentially identical to vegetative peptidoglycan. When the dormant spore germinates, the germ cell wall will serve as the template for the vegetative cell wall (Reviewed in, (85)). Surrounding the germ cell wall is a thick layer

of peptidoglycan known as the cortex. Cortex peptidoglycan features two main modifications as compared to vegetative peptidoglycan, as shown in Figure 1.3. The first is that the cortex is very lightly cross-linked. Peptidoglycan consists of repeating strands of N-acetyl glucosamine (NAG) and N-acetylmuramic (NAM) acid cross-linked by peptide side chains bound to the NAM residues. In vegetative *B. subtilis* approximately 44% of muramic residues are cross-linked to another muramic acid on a separate strand (4). In cortex peptidoglycan, approximately 50% of muramic acid residues are modified to muramic-lactam, which lacks a peptide side chain (75). Nearly 50% of the remaining peptide side chains are cleaved to single L-alanine residues, which also cannot participate in cross-linking (74). These modifications effectively drop the percentage of crosslinks per NAM to 2.4% (5, 62). The low degree of cross-linking may allow the cortex to be significantly more flexible in absorbing mechanical and turgor stress, as an increase in cortex cross-linking has been shown to decrease spore heat resistance (76). Direct reduction of the number of cortex layers has also been shown to decrease the heat resistance of the formed spores (6). During the spore germination process, the cortex must be degraded to allow cell outgrowth. Germination-specific lytic enzymes (GSLEs) recognize muramic lactam and preferentially degrade cortex without harming the germ cell wall (7, 14, 29).

Surrounding the cortex is the spore coat. This layer is composed of two distinct layers comprised mainly of proteins. A number of protective molecules have been identified in the spore coat, including a variant of superoxide dismutase, which protects the cells from exposure to hydrogen peroxide (40).

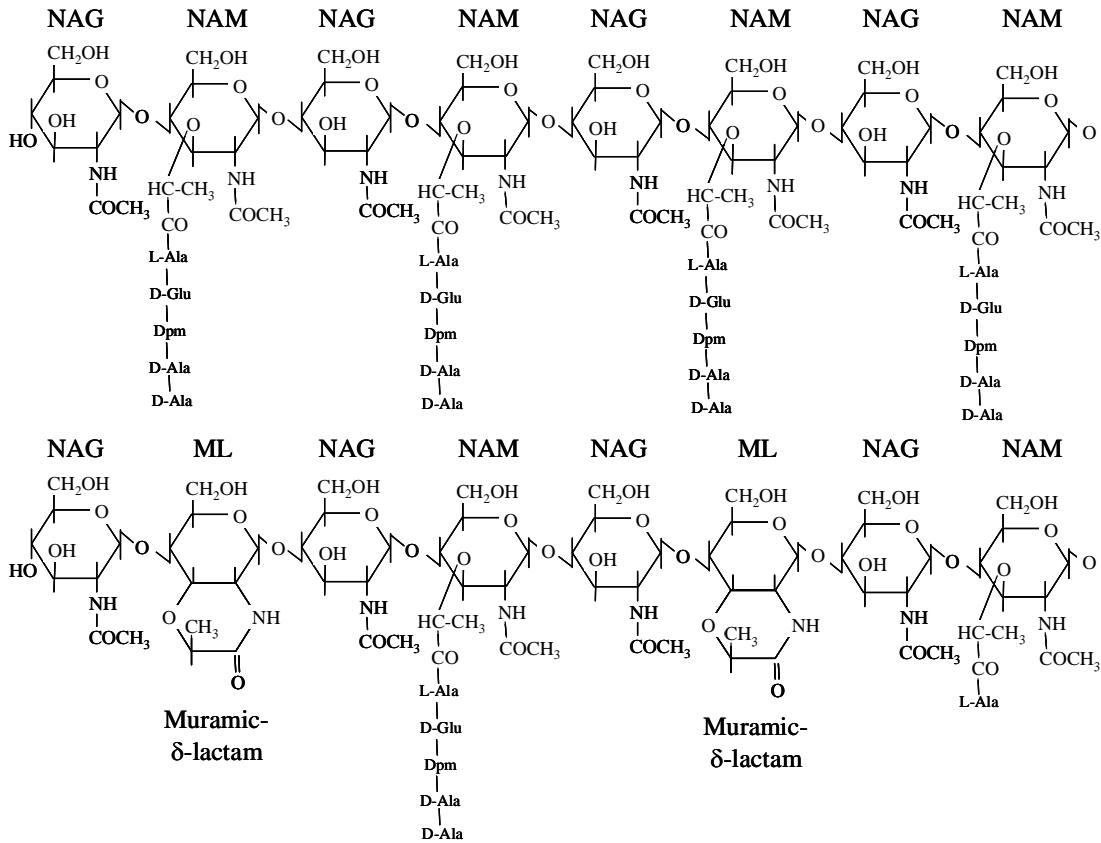


Figure 1.3. Vegetative peptidoglycan structure (top) compared to cortex structure (bottom). N-acetylglucosamine (NAG) is common among both structures as well as L-alanine (L-Ala), D-glutamate (D-Glu) and Diaminopimelate (Dpm). Approximately 50% of the N-acetyl muramic acid (NAM) present in vegetative peptidoglycan is converted to the muramic- δ -lactam that is only present in spore cortex (74).

Analysis of peptidoglycan structure. The structure of *B. subtilis* spore peptidoglycan and comparison with vegetative peptidoglycan was first performed by Warth & Strominger in the early 1970s (100, 101). The method of peptidoglycan extraction has changed little, but advances in separation techniques and analytical chemistry have refined and simplified this process. First, peptidoglycan is removed from bacterial cells by treatments that kill the cells and remove the majority of protein. The peptidoglycan is then digested and solubilized by a lytic enzyme such as lysozyme or mutanolysin. The remaining cellular components are precipitated by centrifugation and

chromatography is performed to separate the soluble muropeptides. The muropeptides are then identified by chemical analysis. Recent techniques rely on HPLC to separate muropeptides and can effectively distinguish between all compounds present on a single gradient, a luxury not available to Warth & Strominger. HPLC separated muropeptides are collected into two pools. The first is acid hydrolyzed and analyzed by amino-sugar and amino-acid analysis to determine the ratio of component subunits. The second is subjected to mass analysis by matrix assisted laser desorption time-of-flight mass spectrometry (MALDI-TOF). The ratio of compounds and the mass value determined allow the determination of the identity of the compound. The original separation of muropeptides is used to quantify the concentrations of each compound and a complete picture of the peptidoglycan structure can be determined (4, 6, 74).

A recent work employed various mass spectrometry techniques to identify novel muropeptides. Using nano-electro spray ionization on a quadrupole mass spectrometer, this group was able to sequentially fragment molecules and successfully determine the structure of a muropeptide without amino-acid or amino-sugar analysis (9). Although still a time consuming process, this study demonstrated that further simplification of solving peptidoglycan structure is possible.

Dipicolinic acid.

Dipicolinic acid (2, 6 –dicarboxylic acid pyridine, DPA) was first identified as a major component of *B. megaterium* spores by Joan Powell in 1953. Within a few years, the literature demonstrated that the spores produced by all known bacteria contained DPA, generally within the range of 5-15% of the spore dry weight (Reviewed in, (99)). Martin and Foster undertook an effort to study the biosynthesis of DPA in *B. megaterium* in 1958 by selectively introducing C¹⁴-labeled compounds to the media or sporulating cells. They determined that two compounds, one 3-C and one 4-C compound condensed to form the carbon backbone of DPA (59).

While studying the production of diaminopimelate in *E.coli*, Yugari and Gilvarg used an *in vitro* assay to determine the product formed by the reaction of L-aspartate semialdehyde and pyruvate catalyzed by *E.coli* whole cell extracts (106). To their surprise, these compounds did not react to form diaminopimelate, but rather condensed to form a cyclic product that rapidly degraded. Chemical analysis of this product determined that it was dihydrodipicolinic acid (DHDPA). Using an assay for the formation of DHDPA, they were able to obtain a partial purification of the enzyme catalyzing this step in *E.coli*, the dihydrodipicolinate synthase (DHDPS) which later became known as DapA (20).

Due to the high similarity of DHDPA to DPA it seemed likely that DHDPA was the direct precursor of DPA. To evaluate this, Bach and Gilvarg undertook a study of DPA production in *B. megaterium* in 1966. In order to study this reaction, whole cell extracts of sporulating *B. megaterium* were assayed *in vitro* with the addition of L-ASA and sodium-pyruvate. DPA formed by this system was removed by extraction with

diethyl-ether and assayed by absorbance at 269 nm. They determined that DPA was not produced by vegetatively growing cells and was only produced by cells late in the sporulation process. They also determined that the lack of pyruvate decreased the production of DPA, but removing L-ASA from the reaction resulted in no DPA production at all, suggesting that the rate-limiting component of this reaction is L-ASA. As L-ASA had been previously implicated as an intermediate in the lysine biosynthesis pathway, DPA was thus implicated as a secondary metabolite of that same pathway (8).

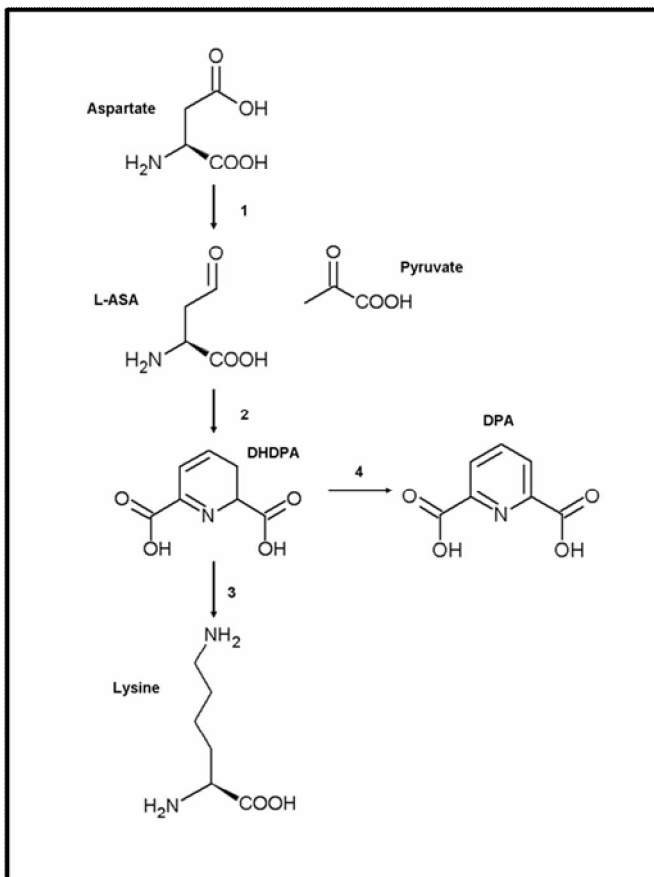


Figure 1.4: Simplified overview of the DPA synthesis pathway. DPA is a secondary metabolite of the lysine synthesis pathway. 1. The two step conversion of aspartate to L-ASA. 2. The condensation of L-ASA and pyruvate to DHDPA catalyzed by DapA. 3. The three step conversion of DHDPA to lysine. 4. DPA synthesis performed by SpoVF in *B.subtilis*.

Many mutant strains of *Bacillus* were identified that lacked production of DPA. The majority of these, however, were also blocked in lysine biosynthesis (36). In 1993, Daniel & Errington cloned a locus from *B. subtilis* into *E. coli* that resulted in a strain that produced DPA (25). Further analysis of this locus revealed that it actually contained two genes, which were termed *spoVFA* and *spoVFB* (21).

Mutant strains of *B. subtilis* lacking DPA were difficult to study, as they were too unstable to survive the purification process. Only the addition of exogenous DPA during sporulation would reverse this phenotype (10). In 2000, work at Peter Setlow's lab developed stable *spoVF* mutant strains. These spores were stabilized by inactivating germinant receptors in a *spoVF*- mutant background. The mutant spores, although stable, possessed spore cores that were significantly less dehydrated than wild-type. The spores were also found to be less resistant to wet heat and UV radiation (69). In vitro analysis of DPA function determined that a chelate of DPA and Ca²⁺ caused an increase in spore photoproduct, a unique characteristic of DNA damage by UV radiation in bacterial spores that is thought to be easily repaired during germination (84). A later study at the Setlow lab isolated another DPA mutant strain. Mutant strains with inactive *spoVA* produced DPA, but did not accumulate DPA in the forming spore. Inactivation of germination receptors allowed the formation of stable spores in this strain, but exogenous DPA did not restore the wild-type phenotype (94). A similar phenotype has been reported in a *C. perfringens spoVA* mutant strain (71).

Several studies have noted the absence of *spoVF* genes in Cluster I clostridia, despite the fact that DPA is known to be present in the spores of these species (1, 66). A survey of 52 organisms representing various branches of the Firmicutes by PCR

amplification of essential sporulation genes found that the only spore forming organisms lacking *spoVF* were members of the Cluster I clostridia (66).

Objectives of this work.

The purpose of the research presented in the following three chapters is to determine what factors are responsible for the resistance of *C. perfringens* spores to wet heat. In Chapter 2, we study the spores produced by nine wild-type strains of *C. perfringens*, including 5 CPE+ and 4 CPE- strains. These spores are analyzed for factors known to affect the heat resistance of spores of other strains, such as core density, DPA and divalent ion content, and spore peptidoglycan structure. The results of this study help to identify what structural criteria must be met by a *C. perfringens* spore to achieve a high level of resistance to wet heat.

To further understand the mechanisms of heat resistance in the spores of *C. perfringens*, we construct mutant strains in a CPE+ *C. perfringens* strain. The genes chosen for inactivation are homologues of genes known to participate in spore maturation and heat resistance in *B. subtilis* spores. The analysis of the spores formed by the mutant strains in Chapter 3 help to support the correlations between the factors identified in Chapter 2 and spore heat resistance.

Chapter 4 details our search for the gene products responsible for the formation of DPA in *C. perfringens*. We develop an *in vitro* assay for the activity of a DPA synthase (DPAS) protein and employ step-wise protein purification of sporulating *C. perfringens* to enrich the DPAS, which is then identified by mass spectrometry. We identify a gene which is essential to DPA formation in *C. perfringens*.

The results of the studies presented in this work will help to explain how *C. perfringens* spores obtain and maintain resistance to wet heat.

Chapter 2

Factors affecting the heat resistance of *Clostridium perfringens* *endospores*

Benjamin Orsburn, Steven B. Melville, and David L. Popham. 2008.

Applied and Environmental Microbiology. 74(11): 3328-3335

ABSTRACT

The endospores formed by strains of Type A *Clostridium perfringens* that produce the *C. perfringens* enterotoxin are known to be more resistant to heat and cold than strains that do not produce this toxin. The high heat resistance of these spores allows them to survive the cooking process, leading to a large number of food-poisoning cases each year. The relative importance of factors contributing to the establishment of heat resistance in this species is currently unknown. The present study examines the spores formed by both CPE+ and CPE- strains for factors known to affect heat resistance in other species. We have found that the concentrations of DPA and metal ions, the size of the spore core, and the protoplast to sporoplast ratio are determining factors affecting heat resistance in these strains. While the overall thickness of the spore peptidoglycan was found to be consistent in all strains, the relative amounts of cortex and germ cell wall peptidoglycan also appear to play a role in the heat resistance of these strains.

INTRODUCTION

The bacterium *Clostridium perfringens* is one of the most common causes of food borne illness in the United States, leading to approximately 248,000 cases each year (61).

Acute food poisoning (AFP) occurs when food is contaminated with *C. perfringens* spores possessing enough heat resistance to survive the cooking process. Rather than killing these spores, the heat stimulates dormant spores to germinate. If the food is not thoroughly refrigerated, the cells then propagate in the food. When this contaminated food is consumed, a large number of the cells survive the low pH of the stomach and begin sporulating in the small intestine. During the sporulation process, the *C. perfringens* enterotoxin (CPE) is produced. This toxin binds to protein receptors found at the intestinal brush border membranes. Several different proteins are involved in the eventual formation of large CPE complexes that cause dramatic changes in membrane permeability, leading to the death of the cell and the symptom of watery diarrhea in the infected individual (reviewed in (60)). *C. perfringens* is also a cause of non-food borne illness, in which the bacterium colonizes the intestinal tract and produces CPE, leading to diarrheal symptoms of longer duration than those found in AFP (15). The *cpe* gene is usually found on the chromosome in strains that cause AFP, while strains that cause non-food borne diarrhea usually carry the *cpe* gene on a plasmid (24).

Two primary bacterial factors contribute to *C. perfringens* AFP. The first is that the contaminating strain produces endospores with a high degree of heat resistance. The second requirement is that the strain must contain and express the *cpe* gene. In an early report, Ando et al., (2) examined five strains of *C. perfringens* that produced highly heat resistant endospores and compared them with five strains that produced spores with

comparably lower heat resistance. This study found that all five of the heat resistant strains expressed the *cpe* gene, while the other strains did not. A recent study by Raju and Sarker (77) compared the heat resistance of CPE+ strain SM101 to that of a derived strain with a *cpe* knockout mutation and found no change in heat resistance was produced by the mutation. It appears that although the expression of the *cpe* gene is associated with more heat resistant strains, the gene or gene product itself does not confer heat resistance.

It has also been noted that the location of the *cpe* gene is associated with the heat resistance of the spores formed by strains of *C. perfringens*. Sarker et al., (81) compared the heat resistance of strains possessing a chromosomal *cpe* gene to the heat resistance of strains carrying a plasmid-borne *cpe* gene. They found that the spores formed by strains with a chromosomal *cpe* gene possessed a decimal reduction value that was, on average, sixty-fold greater at 100°C than the other strains (81). Novak et al., (64) examined the endospores produced by these same strains in an attempt to determine if specific factors could be identified as contributing to this disparity in heat resistance. That study suggested that production of a smaller, potentially more dehydrated spore core was a major factor in determining heat resistance. More recently, Li and McClane (55) showed that strains with chromosomal *cpe* genes are not only more heat resistant but are also more cold resistant in both the vegetative cell and spore forms.

In this study we have examined the endospores of five CPE+ and four CPE- strains to determine what factors contribute to the disparity in heat resistance between these groups. The strains were assayed for heat resistance, protoplast water content, and spore dipicolinic acid (DPA) and mineral concentrations. Spore structural dimensions

were determined using transmission electron microscopy, and the spore cortex structure was determined using liquid chromatography tandem mass spectrometry LC-MS/MS. We have found that CPE+ strains produce spores possessing: smaller core volumes; higher DPA, Ca^{2+} , Fe^{2+} , and Mg^{2+} concentrations; and a lower percentage of tripeptide side chains in the spore cortex than their CPE- counterparts.

MATERIALS AND METHODS

Bacterial strains. CPE + strains: NCTC 8239, NCTC 8679, and NCTC 10240 are food poisoning isolates Hobbs serotypes 3, 6, and 13, respectively (37). SM101 is a derivative of NCTC 8798, Hobbs serotype 9, that is conducive to electroporation (107). Strain 3663 was obtained from the Norwegian Food Research Institute (53). All five CPE+ strains were shown to possess chromosomal *cpe* genes by a duplex PCR method previously described (103), and the expression of CPE was previously verified by immunoblotting (18, 53). CPE- strains: FD-1 and T-65 were originally food isolates (33), but were verified to lack CPE (104). ATCC 3624 and strain 13 are clinical gangrene isolates (37) (88). PCR analysis (103) verified the absence of the *cpe* gene in all four CPE- strains.

Spore preparation and determination of heat resistance parameters. Spores for all strains were prepared in an identical manner by growth at 37°C in Duncan and Strong sporulation media with raffinose (32, 87). In order to increase the sporulation efficiency of the CPE- strains, 0.1% caffeine was added to sporulation media (80). This addition had no apparent effect on the sporulation rate of the CPE+ strains. The heat resistance of the spores of each strain was experimentally determined with and without the addition of caffeine and no measurable difference was observed (data not shown). A variant of strain 13 that sporulates in the presence of phosphate (30) was isolated by growing the cells in DSSM for 72 hours. The cells were concentrated and vegetative cells were killed by the addition of 100 µg/ml lysozyme plus 200 µg/ml trypsin. The surviving spores were used to inoculate the next culture of DSSM and the process was repeated. Surviving spores were saved as the variant strain, 13V1. The variant was found

to produce spores with heat resistance equal to that of the wild type strain (data not shown). Spore heat resistance for all strains was assayed via determination of the decimal reduction value (D value) for each strain at 90°C (2). Samples were removed directly from sporulating cultures 72 hours post inoculation. The samples were heat treated at 70°C for 10 minutes to kill vegetative cells and then assayed immediately. Heat killing of each strain was followed for 4 log reductions in colony forming units (cfu). Heat resistance assays were performed a minimum of five times on at least two separate cultures for each strain.

Spores were purified 72 hours after inoculation. Cultures were harvested by centrifugation at 10,000 x g at 4° C, and vegetative cells were lysed by addition of 100 µg/ml lysozyme plus 200 µg/ml trypsin and incubation at 37°C for 4 hours. SDS was added to a concentration of 1% (w/v) and incubation was continued for an additional hour (64). Removal of SDS and cell debris was accomplished by washing the spore suspension five times with sterile deionized water at 50°C. The spores were verified to be greater than 90% free of vegetative cells by manual counts using phase contrast microscopy.

Determination of spore core water content. Purified spores were assayed for core density using an established density gradient sedimentation method (57). The density gradient material was Histodenz (Sigma), and the gradient range was 75% to 50% w/v Histodenz. Prior to core density determination, spore coats were permeabilized by incubation for 1 hour at 37° C in 1% SDS, 8 M urea, 50 mM DTT, 50 mM Tris-HCl at pH 8.0; followed by four washes with 150 mM NaCl and a final wash in sterile deionized water (76). The effectiveness of the coat permeabilization procedure for each strain was

demonstrated by a greater than three log reduction in cfu upon treatment of the coat permeabilized samples with lysozyme, while lysozyme had no effect prior to permeabilization (data not shown). Permeabilized samples were also plated to verify that the loss in cfu was due to the lysozyme treatment rather than the permeabilization procedure. Each strain was assayed for spore core density a minimum of five times.

Electron microscopy measurements of spore cross sections. Spores were fixed in 1.4% glutaraldehyde, embedded, and sectioned as described previously (52, 64). Transmission electron micrographs were analyzed using Scion Image, release Alpha 4.0.3.2. (Scion Corporation; Frederick, MD). Spore measurements were performed on between 50 and 100 cross sections at 25,000 X magnification. For spore width measurements, non-central cross sections were eliminated from the measured population in two stages. To eliminate sections at an angle through the spore ellipse, spores were discarded that demonstrated a width:length ratio greater than 1.3. In order to eliminate cross sections that were located near the ends of the spores, images were excluded from calculations that possessed a width >1 SD from the mean. Length measurements were subjected to only the second method of exclusion in order to remove measurements of spores that were not centrally sectioned. Spore core (protoplast) volume was calculated by application of the formula for the volume of an ellipsoid; volume = $(4/3)\pi(\text{width}/2)^2(\text{length})$ (12). The protoplast to sporoplast ratio (P/S ratio) was determined as previously described (12).

Dipicolinic acid (DPA) and spore solute concentrations. Spores were suspended to a known optical density at 600 nm (OD_{600}), and DPA was extracted and quantified using an established colorimetric assay to determine the concentration of

DPA/OD₆₀₀ (43). Samples were also plated in triplicate to allow determination of the concentration of DPA/cfu. Spore core volume measurements were applied to this value to determine the concentration of DPA/ μm^3 spore core volume.

Core ion concentrations were determined using inductively coupled plasma spectroscopy (ICP) (91). All tubes, pipette tips, and glassware used in this procedure were first acid washed with 6 N Optima HCl (Fisher). Clean spores were incubated in 200 mM Tris-HCL (pH 8.0) for 20 minutes to release surface-associated ions. Spores were then washed three times in purified H₂O and samples were taken to determine the OD₆₀₀. The spores were then suspended in 1 ml 6 N Optima HCl (Fisher) and heated at 100°C for 30 min. Samples were centrifuged for 15 min at 13,000 rpm, and the supernatant was diluted with fresh deionized H₂O to a final volume of 5 ml. The samples were analyzed with an ICAP 61E simultaneous spectrometer equipped with a Thermo Elemental autosampler. The spectrometer was calibrated with 200 ml 1.2 N Optima HCl (Fisher). The samples were analyzed simultaneously for Ca²⁺, Fe²⁺, K⁺, Mg²⁺, Mn²⁺, and Na⁺. Spore core volume measurements were applied to determine cation concentrations/ μm^3 spore core volume.

Determination of spore cortex structure. Purification of spore peptidoglycan (PG), digestion with muramidase, and separation of muropeptides by HPLC has been previously described (74). Following identification of muropeptide peaks, quantization was performed using integrated peak areas as previously described (74). Muropeptides were collected from the separation of strain SM101 spore PG for analysis via liquid chromatography-electrospray ionization-mass spectrometry (LC-ESI-MS). The LC system was composed of an Agilent 1100 series stack containing a Binary pump, AL8

autosampler, and vacuum degasser system connected in line to the MS. The LC system was used to remove residual phosphate buffer from the original separation and to verify the presence of a single compound collected from the original HPLC fractionation. The LC gradient ran from 0-60% acetonitrile in 0.01% formic acid over a 20 minute run at 200 μ l/min on a HyPurity Aquastar column (2.1 mm x 150 mm, Thermo Electron Corporation).

The mass spectrometer was an ABI/MDS-Sciex 3200 QTrap with a Sciex TurboSpray ion source. For all mucopeptides, the linear ion trap was employed in negative scan mode. The TurboSpray ion source had a voltage of -4500V at a temperature of 250°C. A declustering potential of -50 mV was used for all samples. For MS/MS fragmentations, collision energy was optimized for each individual mucopeptide, but in all cases was between -60 and -120 mV.

RESULTS

Heat resistance and spore core water content. Purified endospores of each strain were heated in water at 90°C and plated to determine viability. The decimal reduction values (D value) at 90°C were computed for each strain (Table 2.1). As expected (2), the CPE+ strains demonstrated consistently higher heat resistance than the CPE- strains. Among the CPE+ strains, two were highly heat resistant with D values >45 minutes, while the other D values were clustered around 20 minutes. The CPE- strains had D values \leq 12 minutes, and the average D value of the CPE+ strains was more than 5 times greater than the average for the CPE- strains.

Spores from each strain were centrifuged on a Histodenz density gradient to determine the spore core wet density (57). The spores with the two highest core densities were also those that possessed the highest D values. The strain with the lowest core density, strain 13, also had the lowest D value. For strains with intermediate D values, there was not a clear relationship between protoplast density and heat resistance.

Table 2.1. *C. perfringens* spore heat resistance and water content^a

Strain	CPE	D value at 90°C	Density (g/ml)	% Water ^b
NCTC 8239	+	120.6±4.5	1.329±0.006	51.6±2.4
NCTC 8679	+	45.6±9.4	1.333±0.008	50.0±3.2
SM101	+	21.4±0.8	1.308±0.004	59.8±1.6
NCTC 10240	+	19.9±2.4	1.308±0.006	59.8±2.4
3663	+	19.0±2.1	1.306±0.010	60.6±3.9
FD1	-	12.5±4.6	1.307±0.006	60.2±2.4
T-65	-	10.1±1.6	1.316±0.006	56.7±2.4
ATCC 3624	-	6.9±0.7	1.322±0.005	54.3±2.0
13	-	5.5±1.6	1.296±0.006	64.6±2.4

^a All values are averages ± standard deviations of at least three determinations using independent spore preparations.

^b Water content was determined using the formula: density = -0.00254x – 1.460 (57) and is expressed as a percent of wet mass.

Spore dimensions and core volume. A large variation in the sizes of spores produced by various strains of *C. perfringens* has been previously noted (64). In order to accurately assay the spore core solute concentrations among our strains, it was necessary to determine the spore core unit volumes. Spores were fixed and examined by thin section electron microscopy. As represented in Figure 2.1, a great deal of structural variation was found in these images. Differences were apparent in core area, cortex width, and coat structure. Several aspects of the spore dimensions were measured (Table 2.2). A two-fold variation in spore core volume was observed among these strains. The three most heat resistant strains, NCTC 8239, NCTC 8679, and SM101 possessed the smallest core diameters and corresponding core volumes, while FD-1 had a much larger

diameter and a core volume over twice as large as those of the smallest strains. Cortex PG thickness also varied, with the thickest cortex present in NCTC 8239, the most heat resistant strain. The next thickest PG layers were in the significantly larger spores of CPE- strains FD-1 and T-65. The thinnest PG was possessed by SM101. The spore coat thickness and structure differed dramatically between these strains, as shown in Figure 2.1. The asymmetrical appearance of the coat in many strains made determination of average coat width difficult to calculate with accuracy (data not shown).

The protoplast to sporoplast ratio (P/S ratio) (12) was determined from these measurements (Table 2.2). The protoplast was defined as the area of the spore within the inner membrane. The sporoplast was determined as the entire area within the outermost layer of PG (12). The lowest P/S ratios were found in the most heat resistant strains, NCTC 8239 and 8679, with values 0.36 and 0.41, respectively. The highest value, 0.49, was demonstrated by CPE- strain FD-1. Among the spore parameters measured, P/S ratio exhibited the strongest relationship with D value across the entire range of CPE+ and CPE- strains (Figure 2.2).

Table 2.2. *C. perfringens* spore dimensions and core volumes

Strains	Core diameter ^a (μm)	Core length ^a (μm)	Core volume ^b (μm^3)	Cortex width ^a (μm)	P/S ratio ^c
NCTC 8239	0.62±0.06	0.72±0.07	0.29	0.13	0.36
NCTC 8679	0.64±0.07	0.79±0.08	0.34	0.10	0.41
SM101	0.63±0.06	0.75±0.08	0.31	0.09	0.49
NCTC 10240	0.68±0.06	0.79±0.07	0.38	0.10	0.46
3663	0.79±0.07	0.89±0.06	0.58	0.10	0.48
FD1	0.83±0.06	0.97±0.08	0.70	0.12	0.49
T65	0.72±0.07	0.96±0.05	0.52	0.12	0.48
ATCC 3624	0.68±0.05	0.89±0.06	0.43	0.11	0.45
13	0.71±0.07	0.87±0.07	0.46	0.11	0.45

^a All values are averages of 50 to 120 measurements \pm standard deviation. The standard deviations for the cortex measurements were found to be ≤ 0.02 in all instances.

^b Spore core volume was calculated by: volume = $(4/3)\pi(\text{width}/2)^2(\text{length})$. (Core length data not shown.)

^cP/S ratio was calculated by dividing the calculated core volume by the volume of the core+PG layer (12).

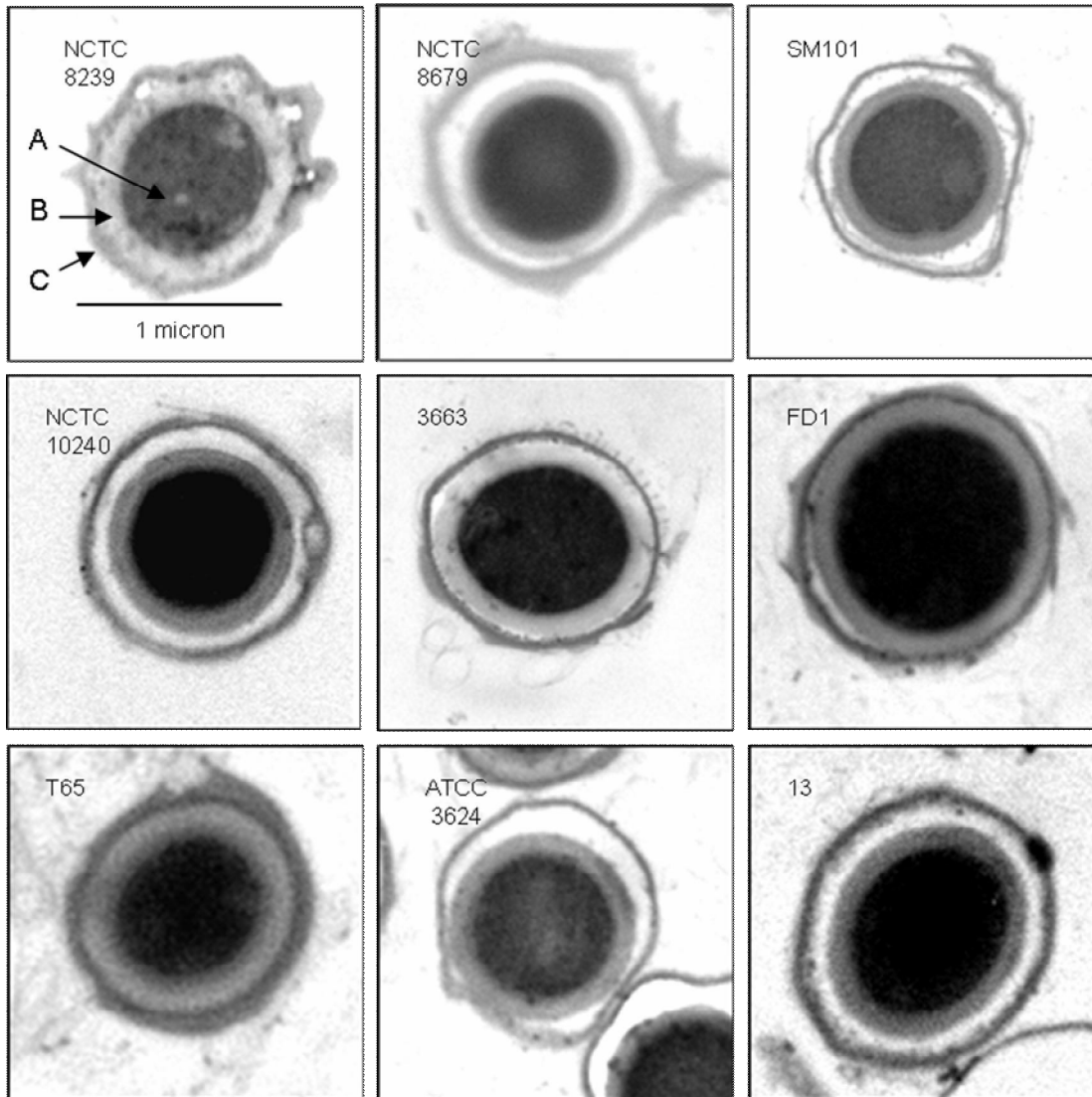


FIG. 2.1. TEM images of *C. perfringens* spore cross sections. Representative images of spores produced by the designated strain are shown in each panel. The scale for each image is the same as that shown in the upper left panel. A, spore core; B, spore PG layer; C, coat layers.

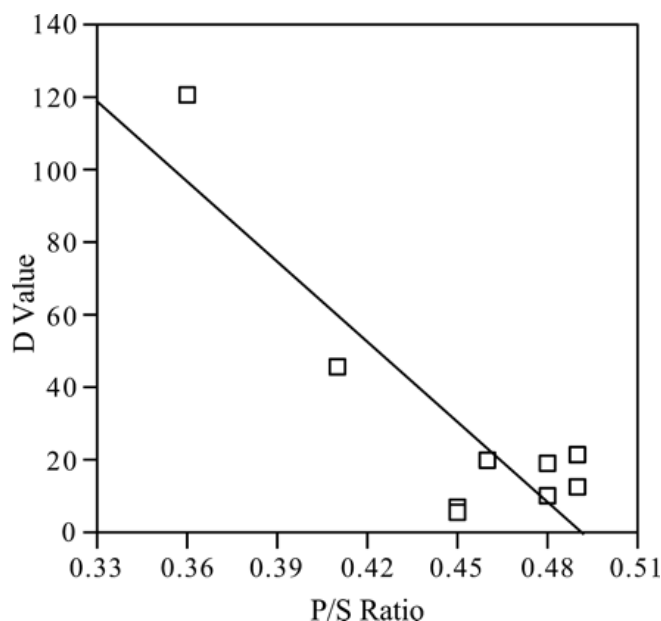


FIG. 2.2. Heat resistance correlates with protoplast:sporoplast ratio in *C. perfringens*. P/S ratio was calculated from measurements of TEM images as previously described (12). The line was drawn using the linear regression method and produced an r^2 value of 0.77.

Spore solute contents. Spore core DPA concentration was determined and was found to differ among strains by as much as 20-fold (Table 2.3). While the average DPA concentration of the CPE+ strains was $65.4 \text{ fmol}/\mu\text{m}^3$, more than twice the average for the CPE- strains, $26.7 \text{ fmol}/\mu\text{m}^3$, an unpaired t test indicated there was no correlation between DPA concentration and D value, (P value = 0.46). Spore monovalent and divalent cation contents were assayed (Table 2.3) with ICP spectroscopy. In all strains, the levels of Na^+ and K^+ were found to be below the limit of detection (data not shown). Ca^{2+} concentration correlated strongly with DPA levels, with an r^2 value of 0.99. The average Ca^{2+} , Fe^{2+} and Mg^{2+} concentrations were more than two-fold higher in the CPE+ strains than in the CPE- strains, with the highest concentration of all four cations found in NCTC 8679. Mn^{2+} concentrations were found to be very similar between the two groups, in the range of $3\text{-}10 \text{ fmol}/\mu\text{m}^3$ (data not shown).

Table 2.3. *C. perfringens* spore solute contents^a

Strain	DPA	Ca ²⁺	Fe ²⁺	Mg ²⁺
NCTC 8239	49.7	41.8	1.8	6.1
NCTC 8679	196.6	130.6	2.3	18.8
SM101	18.9	23.1	0.9	2.1
NCTC 10240	28.9	22.5	0.6	4.3
3663	33.1	25.8	0.8	3.7
FD1	9.0	10.5	0.3	1.2
T65	16.3	14.1	0.2	2.0
ATCC 3624	64.2	51.8	0.7	8.4
13	17.2	14.6	0.5	2.7

^aAll values are averages of 3 measurements on independent spore preparations and are expressed in fmol/ μm^3 .

Spore cortex structure. Spore PG was purified, muramidase digested and analyzed using HPLC. Twenty-one muropeptides were collected from the SM101 sample (Figure 2.3) for structural analysis via ESI-MS/MS. The chromatograms for the other eight strains were very similar to that of SM101, producing a nearly identical series of peaks (data not shown). Eleven of the SM101 muropeptides had elution times closely matching those derived from *Bacillus subtilis* 168 endospores (74), and data not shown) and MS analysis verified the co-eluting peaks to be the same compounds. MS analysis (Figure 2.4A and Table 2.4) revealed that each muropeptide ionized predominantly as a single proton loss (M-H^+) with a lower frequency of Na^+ adducts representing $\text{M+Na}^+-2\text{H}^+$. MS/MS fragmentation was employed on all compounds to determine structures (Table 2.5 and data not shown). In all MS/MS spectra, the saccharide chain fragmented on the non-reducing end of the glycosidic bond to produce primarily Y ions (93). Stepwise assembly of these fragments from the non-reducing end allowed the characterization of the oligosaccharide chain (5). The fragmentation occurring within the peptide side chain followed the well characterized pattern, with both b and y ions present in the same spectra, demonstrating fragmentation of each peptide bond (54). The spore

PG peptide side chain structure was found to be Ala-Glu-Dpm-Ala, the same side chain linkage observed in spores of *Bacillus* species and in *C. botulinum* (6, 99). Unlike the cortex of other endospores previously examined (6, 99), that of *C. perfringens* was found to lack NAM residues possessing single alanine side chains. Dipeptide side chains were present, but at a level nearly 10-fold lower than the percentage of alanine side chains found in other species. Using the structures determined for the mucopeptides, several structural parameters were calculated for the PG extracted from the spores of each strain (Table 2.6). Despite a significantly higher percentage of tetrapeptide side chains, these strains demonstrated a degree of crosslinking lower than that of species previously examined (6). The CPE- strains all possess a greater percentage of tripeptide side chains than the CPE+ strains, with averages of 9.44% and 5.48%, respectively. The highest percentage of tripeptide side chains occurred in FD-1 and ATCC 3624, while the lowest number of tripeptide side chains was found in SM101. Approximately 10% of the N-acetyl glucosamine present in the cortex was found to be deacetylated to glucosamine. This value was fairly consistent in all nine strains.

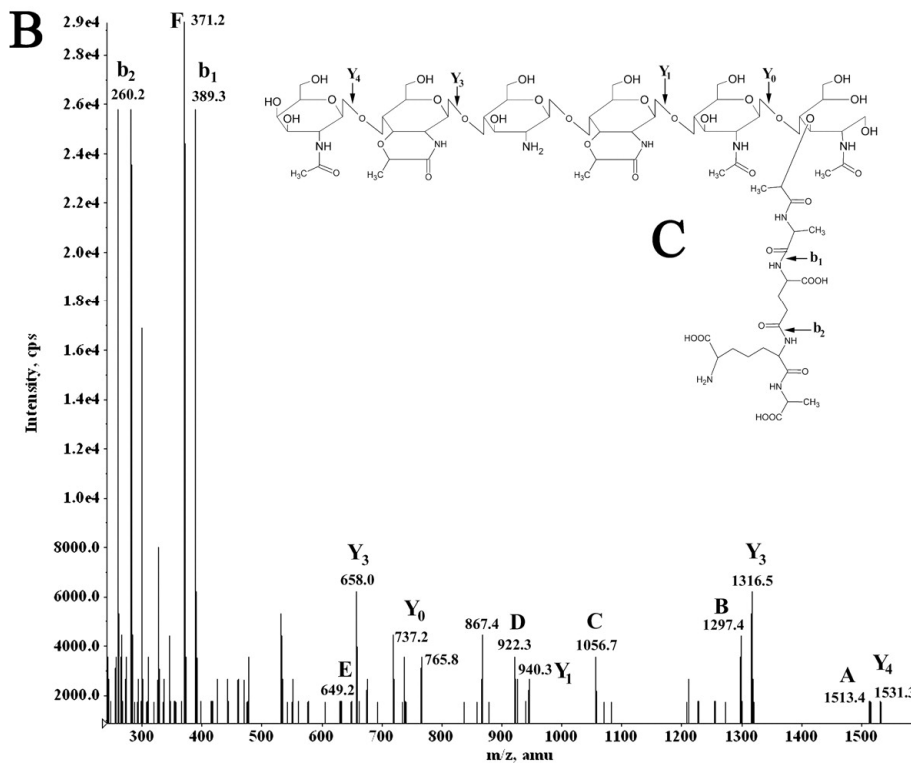
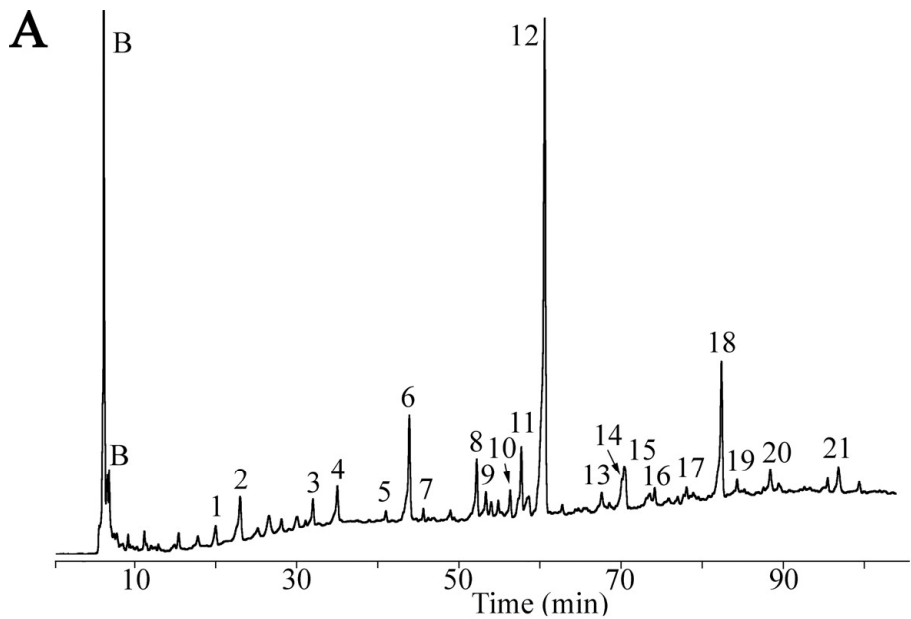


FIG. 2.3. HPLC separation and MS analysis of *C. perfringens* SM101 spore muropeptides. (A) Spore PG was purified, digested with mutanolysin, reduced, and separated using a methanol gradient as previously described (29). Muropeptides were detected by absorbance at 206 nm and are numbered as in Table 2.4. Peaks labeled B are buffer components. (B) Fragmentation spectrum of muropeptide 18. Ion masses indicated by letters are those predicted in panel C and in Table 2.5. (C) Structure proposed for muropeptide 18. The arrows indicate fragmentation points to produce the masses indicated in panel B.

Table 2.4. Muropeptides produced from *C. perfringens* spore PG.

Peak ^a	Predicted Structure	(M-H) ^{-c}	
		Calculated m/z	Observed m/z
1	MS-TP	737.3	737.2
2	DS-TP	940.4	940.4
3	TS-TP (+H ₂ O)	1376.6	1376.4
4	TS-TP(no lactam)	1418.6	1418.6
5	TS(red)-TP(-acetyl)	1302.6	1302.6
6	TS(red)-TP ^d	1344.6	1344.6
7	DS-TriP-DS-TP ^b	1792.7	1792.4
8	TS-TP(-acetyl)	1316.6	1316.4
9	TS-TriP	1288.5	1288.3
10	TS-TP(-acetyl)	1316.6	1316.5
11	HS-TP(-acetyl+H ₂ O)	1752.7	1752.5
12	TS-TP	1358.6	1358.6
13	TS-DP	1115.4	1115.7
14	OS-TP(-two acetyl)	2110.9	2110.4
15	HS(red)-TP(-acetyl)	1720.7	1720.5
16	DS-TP-TS-TP	2281.9	2282.2
17	OS-TP(-two acetyl)	2110.9	2110.6
18	HS-TP(-acetyl)	1734.7	1734.6
19	DS-TriP-TS-TP	2210.9	2211.3
20	TS-TP-TS-TP	2701.7	2702.1
21	HS-TP	1776.7	1776.6

Abbreviations: MS, monosaccharide(NAM); DS, disaccharide; TS, tetrasaccharide; HS, hexasaccharide; OS, octasaccharide; DP, dipeptide (Ala+Glu); TriP, tripeptide (Ala+A₂pm+Glu); TP, tetrapeptide (Ala+A₂pm+Glu+Ala).

^a Peaks are numbered as in Figure 2.4.

^b Indicates a DS-TriP crosslinked to a DS-TP.

^c These masses correspond to the deprotonated molecule in negative ion mode.

^d These are molecules containing reduced (red) muramic lactam. able 5. MS fragment analysis of muropeptide 18.

Table 2.5. Fragment analysis of muropeptide 18.

Fragment ^a	Predicted structure	Predicted m/z (M-H) ⁻	Observed m/z (M-H) ⁻
Y ₄	PS-TP(-acetyl) z=1	1531.3	1531.3
	z=2 ^b	765.2	765.8
Y ₃	TS-TP(-acetyl) z=1	1316.4	1316.5
	z=2 ^b	657.7	658.0
Y ₁	DS-TP	940.4	940.3
Y ₀	MS-TP	736.2	737.2
b ₁	Glu+A ₂ pm+Ala	389.3	389.3
b ₂	Ala+A ₂ pm	260.2	260.2
Products of multiple fragmentation and rearrangements of parent ion.			
A	PS-TP(-acetyl, -H ₂ O) ^c	1513.3	1513.4
B	TS-TP(-acetyl, -H ₂ O) ^c	1297.4	1297.4
C	TS-DP(-acetyl)	1056.4	1056.7
D	DS-TP(-H ₂ O) ^c	922.3	922.3
E	MS-TriP	649.3	649.2
F	Glu+A ₂ pm+Ala(-H ₂ O) ^c	371.1	371.2

Abbreviation: PS, pentasaccharide.

^a List of fragments present in Figure 2.5B and predicted structures that support the proposed structure of compound 18 present in Figure 2.5C.

^b This is a doubly charged ion.

^c The loss of an H₂O, apparently from a cyclization of the peptide side chain, appeared regularly in our fragmentation patterns of this and other previously well-defined muropeptides.

Table 2.6. *C. perfringens* spore PG structural parameters^a

Strain	% muramic acid with:						Deacetylation of NAG
	Lactam ring	No modification ^b	TP	TriP	DP	Cross link	
NCTC 8239	48.7	2.2	38.5	6.4	4.3	1.9	9.2
NCTC 8679	50.0	1.2	38.6	6.2	4.2	1.8	9.6
SM101	50.1	2.0	42.9	3.2	2.4	1.4	11.1
NCTC 10240	49.6	1.8	41.1	4.1	3.6	1.8	9.0
3663	48.2	2.6	37.0	7.5	5.1	1.4	9.5
FD1	47.9	2.5	37.0	11.4	1.6	2.0	9.5
T65	48.3	2.7	37.7	7.9	3.9	1.8	9.0
ATCC 3624	49.6	2.2	34.6	10.3	3.4	1.5	11.0
13	44.3	4.8	40.9	8.2	2.3	1.3	9.2

^a All values are averages of 2 analyses of independent spore preparations. The standard deviation of each value was <5%.

^b Indicates NAM present with no peptide side chain or lactam ring formation.

DISCUSSION

It has long been known that strains of *C. perfringens* that express the *cpe* gene form spores with higher heat resistance than strains that do not express this toxin (2). In this study we selected five CPE+ strains and four CPE- strains of *C. perfringens* and evaluated the spores formed by these strains for factors known to affect heat resistance in other spore-forming species. While all of our CPE+ strains were more heat resistant than the CPE- strains, the division between the groups was not as great as observed previously. The D values at 90°C for our CPE+ strains ranged from 120 to 19 minutes, while those for the CPE- strains were between 13 and 5 minutes. Ando et al., (2) found D values at 95°C from 63 to 17 minutes for CPE+ and 3 to 1 minute for CPE- strains. Sarker et al., (81) determined D values at 100°C of 124 to 30 minutes for strains with chromosomal *cpe* genes and 2 to 1 minute for those with plasmid-borne *cpe* genes. The smaller difference between CPE+ and CPE- strain D values that we observed may be due to the lower temperature we used. We chose 90°C because we found it difficult to obtain accurate D values in the range of 2 to <1 minute at higher temperatures. The broad range of D values across the strains reflects variation in the many factors that can affect heat resistance, as revealed by the measurements of spore structures and contents we obtained.

In *B. subtilis*, mutations or processes that decrease the spore core wet density by increasing the core water content lower the spores' resistance to wet heat (reviewed in (86). Within spores of a single strain prepared under varied conditions and within a set of isogenic strains, this relationship can approach linearity, but between strains and species the results are less uniform, though a general trend is still clear (12). While our most heat resistant strains, NCTC 8239 and NCTC 8679 possessed the highest core densities, and

our least heat resistant strain, 13, had the lowest core density, several other strains varied from this trend. Most notably, CPE- strains ATCC 3624 and T-65 possessed a high degree of dehydration and a lower relative heat resistance. Overall, the average density of the CPE+ strains was very similar to that of the CPE- strains. These results indicate that spore core density is not always a good indicator of heat resistance in this species, and that other factors can play significant roles in determining heat resistance.

A previous study found that the endospores formed by CPE+ *C. perfringens* strains demonstrated a large degree of variation in the core diameter and in the thickness of the cortex and coat layers (64). A similar analysis of our strains supported these findings. While core volume did not appear to correlate with heat resistance over the entire range of our strains, it is worth noting that the three most heat resistant strains possessed the smallest spore core diameters. The average core volume of the CPE+ strains was calculated to be $0.38 \pm 0.12 \mu\text{m}^3$ while the same value for our CPE- strains was $0.53 \pm 0.12 \mu\text{m}^3$. We note that within the CPE+ strains, the thickest cortex belongs to the most heat resistant strain, NCTC 8239. This may reflect the previous observation that across several sporulating species a decrease in the ratio of protoplast to sporoplast volume correlated with an increase in spore heat resistance (12). Among these factors, a low P/S ratio appears to be the most essential to the establishment of heat resistant spores in *C. perfringens*.

In *B. subtilis*, it has been shown that decreasing the amount of DPA in a spore results in reduced heat resistance (33). While this relationship is apparent within a single strain that has been either depleted of DPA (22), or mutated to incorporate less DPA (69), this relationship has never been clearly demonstrated between strains or species. Due to

the large difference in the size of the spores of our strains, it was necessary to standardize the concentrations of the spore solutes and DPA to unit spore core volume to more accurately reflect the presence of these substances. In all nine strains examined, DPA and Ca^{2+} concentrations correlated strongly with one another, with an r^2 value of 0.99. This is not surprising given the strong interaction between Ca^{2+} and the chelator DPA. NCTC 8679 was previously shown to possess extremely high levels of DPA (64), and our results verified this observation. While the average concentrations of DPA and Ca^{2+} among the CPE+ strains were more than twice as high as those among the CPE- strains, the great variability in concentrations within each group resulted in no correlation between these compounds and D values. This suggests that as long as a sufficient level of Ca^{2+} and DPA are present, other factors play greater roles in determining heat resistance.

Spore core Mg^{2+} and Fe^{2+} concentrations were also found to be higher in the CPE+ strains than in CPE- strains. The average Mg^{2+} concentration of the CPE+ strains was nearly twice that of the other strains, while the CPE+ strains had Fe^{2+} concentrations three-fold higher. In *Clostridium botulinum* it was shown that sporulation in iron-deficient media led to production of spores with decreased heat resistance (90), though treatment of spores to incorporate dramatically higher levels of Fe^{2+} also led to a decrease in heat resistance (47). While a mechanism for this phenomenon is not clear, these studies suggested that Fe^{2+} levels in an endospore must remain within a relatively narrow range of concentration, with both increases and decreases outside of this range negatively impacting heat resistance. Strain ATCC 3624 was found to possess a concentration of Fe^{2+} that was relatively low in comparison to those of DPA and the other solutes.

Perhaps this helps to explain why the heat resistance of this CPE- strain is comparatively low, despite its relatively low P/S ratio and high core density.

Cortex PG structure was highly conserved among the nine strains tested and was slightly different from species previously examined (3, 35). The most notable difference from other species is the complete lack of single L-alanine side chains attached to the terminal N-acetyl muramic acid. The enzyme that cleaves peptide side chains to single L-ala in *B. subtilis* is LytH (41), and we could find no gene in the sequenced *C. perfringens* genomes with a high degree of similarity to *lytH*. The result of failure to cleave peptides to single L-alanine residues is a nearly two-fold increase in the number of tetrapeptide side chains in *C. perfringens* compared to other species previously studied (6, 74). Despite the increased number of peptide side chains available for crosslinking, the average percent crosslinking in *C. perfringens* spore PG is ~1.7%; lower than that found in *Bacillus subtilis* (2.4%) (7, 62) and *Bacillus megaterium* (2.2%) (2, 36).

Although many parameters of the cortex structure are very similar among these strains, the abundance of tripeptide side chains is higher in the CPE- strains than in the CPE+ strains; averaging 9.4% and 5.6%, respectively. Strains FD-1 and ATCC 3624 both possess a percentage of tripeptide side chains nearly twice the average of the CPE+ strains. In *B. subtilis*, tripeptide side chains are a characteristic of the germ cell wall rather than the cortex PG (7, 62). A high level of tripeptides in some strains may indicate that a larger percentage of the PG layer measured in our electron micrographs was germ cell wall as opposed to true cortex. This may help to explain the relative thickness of the cortex layers found in the CPE- strains that does not seem to contribute correspondingly to heat resistance.

A novel characteristic of the *C. perfringens* cortex structure is the high degree of de-N-acetylation present in the mucopeptide structure. Nearly 10% of the glucosamine in the cortex was lacking an N-acetyl group, as compared to approximately 3% in *Bacillus megaterium* (5). In the final stage of mucopeptide preparation, the PG was digested with a muramidase. This enzyme cuts adjacent to NAM, but does not act adjacent to muramic- δ -lactam residues. Thus, hexasaccharides result from the presence of two adjacent muramic- δ -lactam residues, and octasaccharides result from three adjacent muramic- δ -lactam residues. It is interesting that while up to ten percent of the tetrasaccharides were deacetylated, the vast majority of the hexasaccharides lacked an acetyl group (data not shown) and 100% of the octasaccharides detected were deacetylated. This suggests that deacetylation of a glucosamine contributes to an increased likelihood of lactam ring formation on the adjacent NAM. The average degree of deacetylation was nearly identical in the CPE+ and CPE- strains and does not appear to be a factor affecting heat resistance in these strains.

Table 2.7 presents a summary of the spore characteristics that appear to correlate with high heat resistance. The mean and standard deviation for each factor was determined based on the values found for all nine strains. If the value for a factor found in a single strain exceeded the mean by 1 SD, the strain is indicated by a '+1'. The two most heat resistant strains, NCTC 8239 and 8679 exceed the mean value in nearly every factor assessed in this study. Every CPE- strain falls more than 1 SD below the mean in at least one category, though this factor is not always the same one. It is interesting that strain FD-1 falls below the mean in every category yet is not the most heat sensitive

strain we assayed. Clearly, other factors contribute to the establishment of heat resistance in this strain.

Table 2.7. Requirements for establishing a highly heat resistant *C. perfringens* spore^a.

Strain	High core density ^b	Small core volume ^c	Low P/S ratio ^d	High DPA ^e	High Fe ^f	PG with low % of TriP ^g	Total
NCTC 8239	+1	+1	+1	+1	+1	0	+5
NCTC 8679	+1	0	+2	+1	+1	0	+5
SM101	0	0	0	0	0	+1	+1
NCTC 10240	0	0	0	0	0	+1	+1
3663	0	-1	0	0	0	0	-1
FD1	0	-1	0	-1	0	-1	-3
T65	0	0	0	0	-1	0	-1
ATCC 3624	0	0	0	+1	0	-1	0
13	-1	0	0	0	0	0	-1

^aEach value is based on the mean value and standard deviation for all strains assayed. A '+1' indicates that the value for that particular strain was above 1 SD but less than 2 SD above the mean. A '-1' indicates a value more than 1 SD but less than 2 SD below the mean.

^bThe mean density for all strains assayed was 1.314 ± 0.012 g/ml.

^cThe mean core volume was 0.44 ± 0.13 μm^3 .

^dThe mean protoplast/sporoplast ratio was 0.45 ± 0.4

^eDue to the outlying DPA content of NCTC 8679 (>2.5SD above the mean), the value was excluded when calculating the mean DPA and Fe content. The mean value for DPA in the remaining strains was 29.7 ± 18.8 fmol/ μm^3 .

^fThe mean value for Fe²⁺ was 0.9 ± 0.7 fmol/ μm^3

^gThe mean value for % TriP was 7.23 ± 2.6

A persistent question in the field remains as to what is the selective advantage to maintaining chromosomal *cpe* genes and the ability to produce highly heat resistant spores. Our first thought is that high heat resistance and accompanying cold resistance (55) is simply a measure of long term stability at ambient temperatures that *C. perfringens* might encounter in the environment (soil and aquatic reservoirs). We then consider that the broad range of *C. perfringens* strains may reflect three separable populations. A population that stably inhabits environmental samples, as opposed to gut flora, are CPE- strains that are the cause of many gas gangrene infections. If these strains

occupy a stable niche in the soil then they may not be selected for CPE expression or for long term spore stability. Another population would be human gut flora isolates, which can be further divided into two classes: $\geq 95\%$ of gut isolates are CPE- and the remainder are CPE+ (26). This subdivision may be determined by a negative selection against CPE by the host immune system and a selective advantage in competition to the small population that maintains CPE. Long term spore stability would then provide a selective advantage for transfer of viable spores between the gut floras of individual host. The advantage would be less for the larger population of CPE- strains which can maintain themselves in a stable population in the gut without stimulating the host immune system, while CPE+ strains would require longer term environmental stability outside of the gut to insure transfer of their smaller population. This could therefore drive the co-inheritance of CPE and high heat resistance. These strains would be frequently encountered in cases of AFP simply due to their ability to survive cooking and refrigeration temperatures. Further insight into the selective factors affecting heat resistance in this species may be obtained by genetically altering a strain to modify these factors within a consistent genetic background.

ACKNOWLEDGEMENTS

The project was supported by the National Research Initiative of the USDA Cooperative State Research, Education and Extension Service, grant number 2004-04069. We thank Katie Sucre for technical assistance and the Soil Testing Lab at Virginia Tech for ICP-Spectroscopy analysis.

Chapter 3

The SpmA/B and DacF Proteins of *Clostridium perfringens*

Play Important Roles in Spore Heat Resistance

Benjamin Orsburn, Katie Sucre, David L. Popham and Steven B. Melville

FEMS Microbiology Letters. **291** (2): 188-194

ABSTRACT

Strains of *Clostridium perfringens* that cause acute food poisoning have been shown to produce spores that are significantly more heat resistant than those of other strains. Previous studies demonstrated that the spore core density and the ratio of spore cortex peptidoglycan relative to germ cell wall were factors that correlated with the heat resistance of a *C. perfringens* spore. To further evaluate these relationships, mutant strains of *C. perfringens* SM101 were constructed with null mutations in *dacF*, encoding a D,D-carboxypeptidase, and in the *spmA-spmB* operon, which is involved in spore core dehydration. The *dacF* mutant was shown to produce less spore cortex peptidoglycan and had a corresponding decrease in spore heat resistance. The *spmA spmB* strain produced highly unstable spores with significantly lower core densities and increased heat sensitivity, which were easily destroyed during treatments affecting the spore coat layers. These results support the previous assertion that a threshold core density as well as a high ratio of cortex peptidoglycan relative to germ cell wall contribute to the formation of a more heat resistant spore in this species.

INTRODUCTION

The bacterium *Clostridium perfringens* is one of the most common causes of acute food poisoning (AFP) each year in the United States. Production of an endospore that possesses enough resistance to wet heat to survive the cooking process is essential for the bacteria to contaminate cooked food and cause AFP. Strains causing AFP have been shown to produce spores that are dramatically more heat resistant than spores produced by other strains of *C. perfringens* (64, 82). We recently studied spores produced by 9 different strains of *C. perfringens* and observed that the most heat resistant spores possessed the highest relative spore core densities, but core density was not an accurate indicator of spore heat resistance except in extreme examples. The protoplast to sporoplast (P/S) ratio, spore solute concentrations and the percentage of tripeptides present in spore peptidoglycan were all factors implicated in heat resistance (29). Another recent study (56) determined that a variant of a small acid soluble protein, Ssp4, was a major determinant of heat resistance. Exchange of the heat resistant Ssp4 variant for one from a heat sensitive strain did not completely negate the heat resistance of that mutant, suggesting that other factors are also involved.

In *Bacillus subtilis*, the *dacB* operon has been shown to be involved in spore resistance to wet heat. The *dacB* gene encodes penicillin binding protein (PBP) 5* (19), which is the primary D,D-carboxypeptidase involved in regulation of spore cortex peptidoglycan cross-linking (74). In *B. subtilis* the *dacB* gene is within a tricistronic operon with the *spmA* and *spmB* genes. The *spm* genes have been shown to be involved in the production of a fully dehydrated spore core (36). Similar to *dacB*, the *B. subtilis*

dacF product is also a D,D-carboxypeptidase that plays a smaller role in regulating cortex cross-linking, and consequently in spore heat resistance (73). In the present study, we have created two mutant strains with inactive *dacF* and *spmA-spmB* genes in *C. perfringens* and demonstrated that these mutations affect spore core density and cortex structure and lead to the development of spores with reduced resistance to wet heat.

METHODS

Bacterial strains. All mutants were constructed in strain SM101, a derivative of strain NCTC 8798 (107). Construction of mutant strains in SM101 by single crossover insertion of a multimeric suicide vector has been previously described (65, 96). Table 3.1 describes the primers used in the construction of these strains.

Table 3.1. Primers used in this study

Name	Primer Sequence	Position ^a
OKS1	CAGTTGGATCCCAAGTATGTTTAAAGAAGGGG	+252 to +285
OKS2	CCTTCTGTCGACGCAACAACACTATTGCAGGTATTG	+768 to +802
OKS3	GCATAATGGATCCCCAGGGAGAGTTGATTACCAC	+113 to +147
OKS4	GATATAACTGTCGACGGAATTAAGTGAATACAAGCTG	+466 to +503
OKS17	GTATGTGAGCTCCAGACCCTAAGCTTTTAGAAATAGGAG	-622 to -583
OKS19	CCAATCCTGCAGTTTTCGTTATTAGCTGCTAC	+1697 to +1728 ^b
DAC1	CGCCTGCAGGTTATTATTTACTAAGTTTGAATC	-180 to -146
DAC2	CGCGGATCCCTCATTATAGATTTTCTTGTTAAA	+1320 to +1354

^aThe position numbering is with respect to the first position in the start codon (+1) of the respective gene.

^bWith respect to the *spmA* +1 site.

^cThe restriction site within each oligonucleotides is underlined.

To create a *dacF* mutant a 550 bp internal region of the gene was amplified by PCR with oligonucleotides OKS1 and OKS2. The PCR product was digested with *Bam*HI and *Sal*II and ligated to similarly digested plasmid pSM300 to produce plasmid pKS3. pSM300 carries an *ermBP* gene, which confers erythromycin resistance to both *C. perfringens* and *E. coli*, but possesses only an *E. coli* origin of replication (65). pKS3 was transformed into the RecA⁺ *E. coli* strain JM107 by electroporation to produce multimeric forms of pKS3 (96). Multimeric pKS3 was introduced by electroporation into SM101 and transformants selected by plating with 30 µg/mL erythromycin. Southern blot analysis was performed to verify disruption of the *dacF* gene (data not shown). An identical strategy was performed to create strain KS2, the *spmA*-*spmB* mutant strain, except primers OKS3 and OKS4 were used to amplify a 409 bp sequence internal to the

spmA gene and this fragment was ligated into pSM300 to form pKS4. The *spmA* gene is predicted to lie in a bicistronic operon with the *spmB* gene. RT-PCR analysis indicated that both the *spmA* and *spmB* genes were effectively inactivated by this multimeric insertion (data not shown). The *spmA*-*spmB* complemented strain was constructed by using primers OKS17 and OKS19 to amplify a 2.3-kb region including the two genes. The PCR product was digested with *SacI* and *PstI* and ligated into pJIR750, an *E. coli* - *C. perfringens* shuttle vector, to produce plasmid pSPM1. The *dacF* complemented strain was constructed using primers DAC1 and DAC2 to amplify a 1.5 kb region; the PCR product was digested with *BamHI* and *PstI* and ligated to pJIR750 to create plasmid pDAC4. Complementing plasmids were transformed into the mutant strains by electroporation and transformants were selected by growth on PGY plates (29) containing 30 µg/mL erythromycin and 20 µg/mL chloramphenicol.

Spore preparation and determination of D values. Isolated colonies of each strain were suspended in fluid thioglycollate medium (FTG) plus the appropriate antibiotics and grown overnight. Spores were obtained by inoculating from the FTG culture into DSSM medium plus 1 mg/ml caffeine to stimulate spore formation (32, 80). Sporulating cultures were sampled for determination of heat resistance parameters at 72 hours post inoculation. Five mL samples were removed and heated at 70°C for 10 min to kill vegetative cells. The heat-treated samples were separated into 200 µL aliquots and heated at 90°C in a mineral oil bath. At five min intervals the aliquots were removed and serially diluted in sterile distilled water. The dilutions were spread on PGY plates and incubated anaerobically at 37°C for 24 hours for colony forming units (cfu) determination. The D value, or the amount of time necessary to reduce viable counts by

one log value, for each time point was determined by use of the formula: $D = U / (\log b - \log a)$, where U = the total time of heating, b = initial cfu count, and a = the number of surviving spores at that time point (102). Each sample was followed for a time equal to a 3 log drop in initial cfu.

Purified spores were obtained as previously described (64, 67) and were verified to be >95% free spores by phase contrast microscopy. As the spores formed by the *spmA-spmB* mutant were found to be highly unstable (data not shown), spore preps were purified and assays were performed on the same day.

Determination of spore density. Purified spores were centrifuged on a 70% to 50% Histodenz (Sigma) gradient to determine spore density (57). Spores formed by the *spmA-spmB* mutant strain were found to lyse during the coat permeabilization process (data not shown) so all strains were assayed without the coat permeabilization step previously described (67). Spore density measurements were performed a minimum of 4 times for each strain.

Electron microscopy of spore cross sections. Spores were fixed in 1.4% glutaraldehyde, embedded, and sectioned as described previously (19, 31). Transmission electron micrographs were analyzed as previously described (12, 67).

Dipicolinic acid (DPA) and spore solute concentrations. DPA concentrations were determined by a colorimetric assay (43). In order to achieve complete release of spore DPA, 1 mL samples of clean spores at an OD_{600} of 10 were placed into 2 mL screw cap centrifuge tubes (Fisher) and autoclaved at 121°C for 25 minutes. A separate aliquot of each spore prep was heated at 70°C for 5 min to stimulate germination and plated on PGY medium to determine OD_{600}/cfu . DPA in fmol/cfu was then calculated. Spore core

solute concentrations were determined by atomic flame absorption spectroscopy (67) and the values obtained were converted by the same method as described above for DPA to fmol/cfu.

Determination of spore peptidoglycan structure. Purification of spore peptidoglycan, digestion with muramidase, and separation and quantization of muropeptides by HPLC has been previously described (74). As the strains evaluated here produced the same elution pattern as SM101, the muropeptides from this strain were identified by co-chromatography with the compounds previously identified from SM101 (67).

Statistical analysis. All statistical tests were run with GraphPad InStat, version 3.0b for Macintosh; Graph Pad Software, San Diego, California.

RESULTS AND DISCUSSION

Identification of *dac* and *spm* homologues. A search of the *C. perfringens* SM101 genome revealed only single predicted gene products with similarity to *B. subtilis* SpmA and SpmB. CPR2542 has 39% identity to *B. subtilis* SpmA over an alignment of 174 residues of the 192 amino acid *C. perfringens* and 196 amino acid *B. subtilis* proteins. CPR2541 has 40% identity to *B. subtilis* SpmB over an alignment of 167 residues of the 172 amino acid *C. perfringens* and 179 amino acid *B. subtilis* proteins. The *C. perfringens* *spmAB* genes are in an apparent operon, as *spmAB* are in *B. subtilis*. Single sets of nearly identical genes were found in the other available *C. perfringens* genome sequences as well as in other spore forming organisms.

Similar results were obtained in searches of each of the available *C. perfringens* genome sequences for homologues of *B. subtilis* DacB and DacF. Four genes with significant similarity were found in each genome. We chose to study CPR1775 (402 amino acids), which has 44% sequence identity and 69% similarity over an alignment of 344 of the 389 amino acids of *B. subtilis* DacF. In *B. subtilis*, *dacF* is expressed on the forespore side of the asymmetric sporulation septum, from a sigma F-dependent promoter (45, 54). We examined the sequences upstream of CPR1775 for matches to *B. subtilis* consensus sequences (39) and identified a strong candidate sigma F-dependent promoter (GCTTA-16-GGAGAAAATA-21-ATG).

Heat resistance and spore stability. Insertional mutations in both *dacF* and *spmA* in the SM101 background were isolated, and mutant strains carrying complementing plasmids were constructed. Sporulating cultures for each strain, SM101, the *dacF* mutant, the *spmA-spmB* mutant, and their respective complemented strains were

assayed for D values at 90°C (Table 3.2). The *dacF* mutant spores demonstrated a minor, though statistically significant, decrease in heat resistance ($P= 0.022$). The *spmA*-*spmB* mutant spores were found to be much less heat resistant than those of the wild type with a D value reduced 5-fold. Complementation of each mutation using plasmid-borne genes restored full spore heat resistance.

Table 3.2. Spore heat resistance and wet density.

Strain	D value at 90°C (min) ^a	Density (g/ml) ^a
SM101	22.1±2.4	1.258±0.005
<i>dacF::erm</i>	17.8±1.7	1.252±0.007
<i>dacF::erm</i> pDAC4:: <i>cm</i>	20.3±1.4	1.256±0.004
<i>spmA::erm</i>	4.1±1.6	1.235±0.006
<i>spmA::erm</i> pSPM1:: <i>cm</i>	23.6±4.5	1.255±0.004

^a All values are averages ± standard deviations of at least three determinations using independent spore preparations.

In *Bacillus subtilis* the *dacB*, *spmA*, and *spmB* genes occupy a three gene operon (76). Insertional deactivation of any of these genes has been shown to decrease spore resistance to wet heat. In *B. subtilis*, an in-frame Δ *dacB* mutation resulted in an approximate 5-fold decrease in heat resistance at 85°C, while inactivation of either the *spmA* or *spmB* genes resulted in a 7-fold decrease (36). Inactivation of *dacF* alone in *B. subtilis* resulted in no significant alteration of spore heat resistance (34, 54), though the additional loss of *dacF* in a *dacB* mutant further reduced heat resistance, revealing the role of *dacF* in that species (73, 105). While both of our mutants produced spores with reduced resistance to wet heat, the *dacF* mutant suffers only a minor reduction compared to the *spmA*-*spmB* mutant.

Loss of *dacB* in *C. perfringens* also resulted in a decrease in heat resistance (70), but it is difficult to compare the relative level of change in heat resistance to what we observed in a *dacF* mutant. Previous reports on the heat resistance of the spores formed

by SM101 have reported inconsistent D values at 100°C (37) with values ranging from 49 (70) to 90 minutes (78). We have found D values at 90°C to be highly consistent over a 4 log drop in cfu in over 20 separate assays (67).

Spore density. Spores from each strain were centrifuged on a Histodenz gradient to determine spore density (57). While *dacF* mutant spores were found to be very similar to the wild-type, *spmA-spmB* spores were significantly less dense than wild-type spores ($P=0.031$). Complementation of the *spmA-spmB* mutant resulted in a full restoration of spore density (Table 3.2). These results are consistent with results recently obtained for a *spmA-spmB* and *dacB* mutant (70).

Spore dimensions and core volume. Spore cross sections were examined by TEM as previously described (67). As shown in Figure 3.1 and Table 3.3, spores formed by the *dacF* mutant were consistently found to possess significantly smaller spore core volumes and thinner peptidoglycan layers than wild-type strains ($P<0.001$, for both measurements). The *dacF* mutant also demonstrated a significantly higher P/S ratio than the wild-type ($P<0.01$). It has been shown for many species that lower P/S values correspond with increased heat resistance (Beaman *et. al.*, 1982). Complementation of this strain with the plasmid-borne *dacF* gene completely restored the wild-type structural phenotype (Table 3.3).

Spores from the *spmA-spmB* mutant strain could not be examined by TEM. The spores were shown to be too unstable to survive the fixing process as demonstrated by a >60% decrease in phase bright spores following treatment with glutaraldehyde (data not shown). Complementation of the *spmA-spmB* genes restored spore stability following

treatment with glutaraldehyde and spores were not found to differ significantly from the wild-type (Table 3.3).

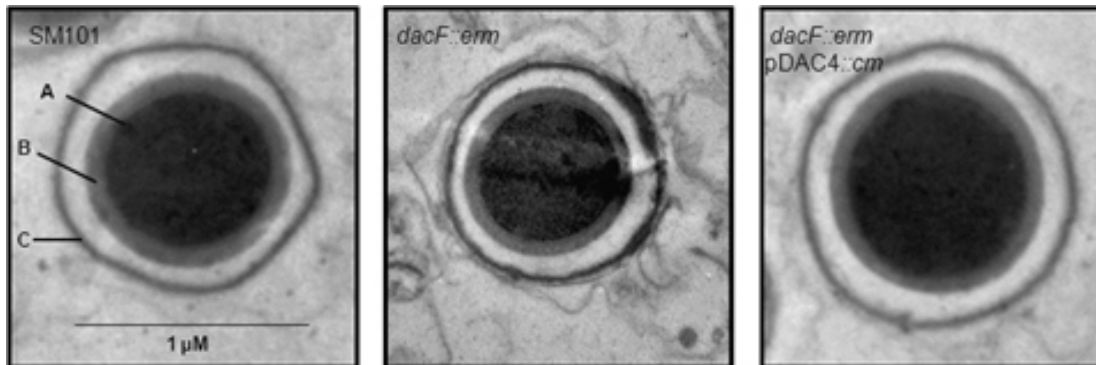


Fig. 3.1. TEM images of *C. perfringens* spore cross sections. Representative images of spores produced by SM101 (left panel), the *dacF* mutant strain (center panel), and the complemented *dacF* mutant (right panel). The scale for each image is the same as that shown in the left panel. (A) Spore core. (B) Spore peptidoglycan layer. (C) Coat layers.

Table 3.3. *C. perfringens* spore dimensions and core volumes

Strains	Core diameter ^a (μm)	Core length ^a (μm)	Core volume ^b (μm ³)	Cortex width ^a (μm)	P/S ratio ^c
SM101	0.65±0.04	0.72±0.11	0.32±0.06	0.09±0.02	0.49±0.10
<i>dacF::erm</i>	0.54±0.05	0.73±0.09	0.22±0.04	0.05±0.02	0.63±0.14
<i>dacF::erm</i> pDAC4::cm	0.66±0.03	0.74±0.10	0.34±0.05	0.10±0.01	0.46±0.08
<i>spmA::erm</i> pSPM1::cm	0.61±0.06	0.88±0.07	0.34±0.05	0.10±0.02	0.46±0.09

^a All values are averages of 50 to 80 measurements ± standard deviation.

^b Spore core volume was calculated by: volume = (4/3)π(width/2)²(length).

^c P/S ratio was calculated by dividing the calculated core volume by the volume of the core+peptidoglycan layer (12).

DPA and spore solute concentrations. Spore DPA and levels of Ca²⁺, Fe²⁺ and Mg²⁺ were determined as previously described (67). Both mutant strains demonstrated reduced levels of spore core DPA and Ca²⁺ compared to the wild-type, with the most pronounced difference apparent in the *spmA-spmB* mutant (Table 3.4). While DPA and Ca²⁺ levels appear lower per cfu for the *dacF* mutant strain, it is worth noting that the reduced core volume of the *dacF* mutant spores may be responsible for the reduced

value. If the spore core DPA levels are divided by the calculated spore core volumes in Table 3.3, the values for the wild-type and *dacF* mutant spores are 17.6 fmol and 16.0 fmol/ μm^3 , respectively. Complementation of the *spmA-spmB* mutant restored most of the DPA and Ca^{2+} , but did not achieve wild-type levels.

Table 3.4. *C. perfringens* spore solute contents^a

Strain	DPA	Ca^{2+}	Fe^{2+}	Mg^{2+}
SM101	5.1±1.3	5.7±0.6	0.2±0.1	0.2±0.1
<i>dacF::erm</i>	3.9±0.9	4.7±1.7	0.3±0.1	0.2±0.1
<i>dacF::erm pDAC4::cm</i>	4.6±1.1	4.2±0.2	0.3±0.1	0.3±0.1
<i>spmA::erm</i>	1.7±0.5	2.0±0.9	0.7±0.1	0.5±0.2
<i>spmA::erm pSPM1::cm</i>	4.2±0.7	4.7±0.4	0.2±0.1	0.2±0.1

^aAll values are averages of 3 measurements on independent spore preparations and are expressed in fmol/cfu.

The *spmA-spmB* mutant spores demonstrated higher levels of Fe^{2+} and Mg^{2+} than the wild-type strains. Spore solute values obtained for the *spmA-spmB* mutant may be affected by the relative instability of these spores. It is quite possible that the spores initially accumulate Ca^{2+} and DPA, but lose it during spore purification. The apparent high levels of Fe^{2+} and Mg^{2+} could be due to the reduced cfu counts found for this strain. As the wild-type strain requires a short heat treatment to effectively stimulate germination, the spores of all strains were heated at 70°C for 5 min prior to plating to determine cfu. Due to the extreme heat-sensitivity of the spores formed by the *spmA-spmB* mutant strain, a number of spores may have died during this treatment, providing an artificially repressed cfu count, consequently increasing this value. If this is indeed true, it suggests that the low Ca^{2+} and DPA contents may also be an overestimate of that actually present. Whatever the true content values of these solutes, these values suggest that the mechanism(s) of accumulation and/or maintenance of Fe^{2+} and Mg^{2+} is different

than that for Ca^{2+} and DPA, as these solute pools respond in opposite manners to the *spmA-spmB* mutation.

Stability of the *spmA-spmB* spores. The *spmA-spmB* mutant strain was found to produce highly unstable spores which demonstrated decreased cfu counts when stored at both 4°C and 37°C. The number of viable spores decreased by nearly 1 log drop every 5 days until reaching a stable number of spores representing a >3 log reduction in initial cfu. By use of a chemical method to remove vegetative cells (64), we were able to harvest spores and begin assays on the same day. This enabled us to obtain a more accurate picture of the total spore population and the true *spmA-spmB* phenotype, and not just the stable subpopulation. A recent study analyzed NM101, a similar *spmA-spmB* mutant constructed in an SM101 background (70). NM101 spores were cleaned by repeated washes and centrifugations, a method that requires several days to obtain clean spore preps (63). When the spores were verified to be clean by microscopy, they were diluted to a constant OD₆₀₀ and frozen. The cells were then thawed and assayed. The NM101 strain was not reported to be unstable, neither during storage, nor during the decoating process used prior to the density assay performed. This may be due to the unstable population being removed by the repeated water washes necessary to obtain clean spores. Likewise, NM101 strain was not shown to exhibit the drastic decrease in DPA that we report for our strain. This also may be due to the loss of the spores exhibiting the unstable *spmA-spmB* phenotype.

Analysis of spore cortex structure. The spores of both the *spmA-spmB* mutant and the complemented strain contained a peptidoglycan structure that was highly similar to the wild-type (Table 3.5). However, the *dacF* mutant differed from the wild-type as

follows: an increase in the abundance of tripeptide side chains, a reduced percentage of lactam ring formation, and an increase in cross-linked compounds. A *B. subtilis dacF* mutant had no significant change in cortex structure, whereas a $\Delta dacB$ mutant was shown to possess a dramatic increase in cross-linked muropeptides (73). These effects of the *B. subtilis* Dac proteins correlated well with their effects on spore heat resistance. Similarly, the *C. perfringens dacF* mutant presented here does show an increase in tripeptide and cross-linked muropeptides, though the changes are not nearly as dramatic as those found in the *B. subtilis* $\Delta dacB$ mutant (36). This may reflect slightly different roles played by these gene products in the two species, with *C. perfringens* DacF playing a more significant role than that of DacF in *B. subtilis*. The different effects of DacF could depend on a number of differences between the peptidoglycan of *C. perfringens* and *B. subtilis* spores. In *B. subtilis*, nearly 50% of the peptide side chains are cleaved to single L-alanine residues by the LytH enzyme (41). The lack of this enzyme in *C. perfringens* results in a dramatically higher percentage of tetrapeptide side chains. Despite the high number of these side chains that should be able to participate in forming peptide cross-links, all nine *C. perfringens* strains studied demonstrated a percent cross-linking lower than that of *B. subtilis* (67). Although little is known of the mechanisms leading to spore peptidoglycan formation in *C. perfringens* it appears that it differs from the characterized *Bacillus* species in several regards. The construction of further mutant strains will be necessary to determine how the sporulation process actually proceeds in this species.

Table 3.5. Biochemical characterization of the PG of *C. perfringens* spores^a

Strain	% muramic acid with:					Cross link	Deacetylation of NAG
	Lactam ring	No modification ^b	TP ^c	TriP ^d	DP ^e		
SM101	49.9	2.2	42.9	2.9	2.1	1.5	11.4
<i>dacF::erm</i>	44.6	4.8	45.1	4.1	1.4	2.1	10.9
<i>dacF::erm pDAC4::cm</i>	50.1	2.3	44.1	2.5	1.0	1.5	13.3
<i>spmA::erm</i>	50.9	2.5	42.0	3.0	1.7	1.5	11.7
<i>spmA::erm pSPM1::cm</i>	49.6	2.0	43.5	3.4	1.8	1.6	11.5

^a All values are averages of 2 analyses of independent spore preparations. The variation of each value was <5%.

^b Indicates NAM present with no peptide side chain or lactam ring formation.

^cTP, Tetrapeptide (Ala + Glu + A₂pm + Ala)

^dTriP, Tripeptide (Ala + Glu + A₂pm)

^eDiP, Dipeptide (Ala + A₂pm)

ACKNOWLEDGEMENTS

This project was supported by the National Research Initiative of the USDA Cooperative State Research, Education and Extension Service, grant number 2004-04069.

We thank Wes Black and Kathryn Harry for helpful discussions.

Chapter 4

EtfA is essential for DPA production in *Clostridium perfringens*

Benjamin C. Orsburn, Steven B. Melville and David L. Popham

ABSTRACT

Dipicolinic acid (DPA) is a major component of bacterial endospores, generally comprising 5-15% of the spore dry weight. DPA has been shown to protect spores from killing due to dry heat. In bacteria and plants, dihydro-DPA (DHDPA) is produced by DHDPA synthase as an intermediate of the lysine biosynthesis pathway. In *Bacillus subtilis*, and certainly in most other bacilli and clostridia, DHDPA is oxidized to DPA by the products of the *spoVF* operon. Analysis of the genomes of the clostridia in Cluster I, including the pathogens *C. perfringens*, *C. botulinum*, and *C. tetani* has shown that no *spoVF* orthologs exist in these organisms. Using an *in vitro* assay, DPA synthase activity was purified 100-fold from extracts of sporulating *C. perfringens*. Peptide sequencing by mass spectrometry implicated an electron transfer flavoprotein, EtfA. A mutant strain was constructed with an insertional inactivation of *etfA*. This strain is blocked in late stage sporulation and produces only 11% of wild-type DPA levels. *C. perfringens* EtfA was expressed in and purified from *E. coli*, and this protein was shown to participate in DPA formation *in vitro*. The sequential production of DHDPA and DPA in *C. perfringens* appears to be catalyzed by DHDPA synthase with the second step requiring the participation of EtfA. As the spore is commonly the infectious agent in diseases caused by the Cluster I clostridia, this study may lead to novel approaches for the prevention of these conditions.

INTRODUCTION

Dipicolinic acid (DPA) is a major component of all bacterial endospores, comprising 5-15% of the spore dry weight (69). Mutant strains that are deficient in production of DPA or its accumulation into the developing spore produce spores with decreased stability and resistance to wet heat (58, 69). In *Bacillus subtilis*, DPA is produced during late stage sporulation via a branch off the lysine biosynthetic pathway. One step in this pathway is catalyzed by dihydro-dipicolinate synthase (DHDPS) which is encoded by *dapA*, and disruption of this gene results in the formation of spores deficient in DPA (25, 92). DHDPS has long been thought to condense aspartate semialdehyde (L-ASA) and pyruvate to produce dihydrodipicolinate (DHDPA) (106)(Figure 4.1). Analysis of the reaction catalyzed by DHDPS using NMR spectroscopy has suggested that the product of this enzyme is not DHDPA, but rather 4-hydroxy-tetrahydro-dipicolinic acid, which may undergo spontaneous dehydration to DHDPA (16). Production of DPA from L-ASA and pyruvate *in vitro* has been accomplished with a sporulating cell extract (8), apparently requiring the presence of both a DHDPS and a DPA synthase (DPAS). The latter enzyme is the product of the *spoVF* operon, which produces two products; *spoVFA* encodes a putative dehydrogenase, while the *spoVFB* product appears to be a flavoprotein. Inactivation of either gene in *B. subtilis* resulted in loss of DPA production, and expression of both genes in *E. coli* under conditions that induce lysine biosynthesis resulted in DPA synthesis (25).

Genome sequence analysis has shown that members of the Cluster I clostridia, including *C. perfringens*, *C. botulinum*, *C. tetani*, *C. acetobutylicum*, and *C. beijerinckii* lack genes with significant homology to *spoVF* (50), yet are known to produce DPA

during sporulation (72). The lack of this enzyme does not appear to extend beyond Cluster I, as genome sequence analyses indicate that both *C. difficile* in Cluster XIa and *C. phytofermentans* in Cluster XIVa (98), possess clear homologues of *spoVF*. In order to identify the enzyme responsible for the formation of DPA in *C. perfringens* we developed a modified version of the Bach & Gilvarg assay system (8) purified the DPAS activity, and identified protein in the purified fraction. We have determined that CPR_2284, which encodes an electron transfer flavoprotein α -chain (EtfA), is directly involved in DPA synthesis in *C. perfringens* and is likely to be important in this process in the other Cluster I clostridia.

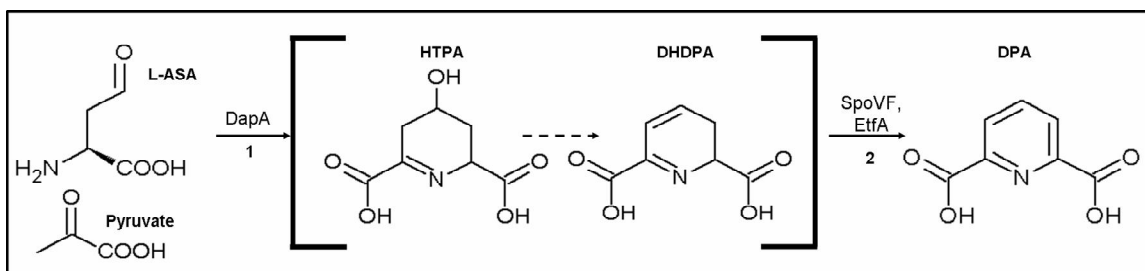


Figure 4.1. Mechanism of DPA formation. L-ASA, HTPA and DHDPA are intermediates of the lysine biosynthesis pathway. Reaction 1, the condensation of L-ASA and pyruvate is catalyzed by DapA (DHDPS). The conversion of HTPA to DHDPA is thought to occur by a spontaneous dehydration reaction and is represented with the dotted arrow. Reaction 2, the conversion of DHDPA to DPA is performed by SpoVF in *B. subtilis* and appears to be performed by EtfA in *C. perfringens*.

RESULTS AND DISCUSSION

Purification of the *C. perfringens* DPA synthase. *C. perfringens* and other Cluster I Clostridia do not possess homologues of the characterized DPAS of the Bacilli. The assay used for purification of DPAS activity included L-ASA, pyruvate, and a source of DHDPS activity. Previous similar *in vitro* studies in which DPA was detected by absorbance at 269 nm suggested that DPA may form spontaneously at high pH (48, 49). Analysis of the products of our activity assays with multiple reaction monitoring (MRM) mass spectrometry demonstrated that negligible DPA was formed in the presence of a cell extract containing DHDPS alone. While an increase in absorbance at 269 nm was observed, it was significantly greater than that expected from the amount of DPA produced. These results strongly suggest that a DPAS is required to produce DPA at the physiologically relevant conditions present in our assay.

Analysis of whole cell extracts of NCTC 8679, a strain shown to produce spores with high DPA concentration (67), indicated that DPAS activity in this strain was greatest 11 hours after inoculation into DSSM. A summary of the purification of DPAS from cells at this stage is shown in Table 4.1. The whole cell extract was first separated into five fractions by ammonium sulfate ((NH₄)₂SO₄) precipitation. Unlike the whole cell extract, none of the fractions were capable of producing DPA alone. Only the 55-70% ((NH₄)₂SO₄) fraction was capable of producing DPA when added to a crude extract of *B. subtilis* strain FB106 (*spoVF::tet*)(69) as the source of DHDPS. To determine which ((NH₄)₂SO₄) fraction contained the *C. perfringens* DHDPS, each fraction was mixed with the others for assay. The combination of the 40-55% and 55-70% ((NH₄)₂SO₄) fractions resulted in DPA formation, indicating that the 40-55% ((NH₄)₂SO₄) fraction contained

the DHDPS (data not shown). Further fractionation using ion exchange and size exclusion chromatography was performed on the 55-70% ((NH₄)₂SO₄) fraction, and the *in vitro* assay was performed using the 40-55% ((NH₄)₂SO₄) fraction as a source of enriched DHDPS. The final, most active DPAS fraction was separated using both native and denaturing SDS-PAGE, revealing the presence of 10-20 protein species. Slices were excised from the native gel and subjected to the assay system.

Table 4.1. Purification of the DPA synthase of *C. perfringens*

Fraction	Total protein mg	Specific activity µg DPA/mg(min)	Yield %	Fold purified
Crude extract	901	0.08	100.0	1.0
55-70% (NH ₄) ₂ SO ₄	172	0.38	85.8	4.5
HiTrap QXL	13	1.45	24.6	17.0
Superdex 200	1.8	8.62	20.3	102

Peptide sequencing results. MALDI-TOF/TOF peptide sequencing identified five proteins that were present in the native-PAGE gel slices exhibiting DPAS activity. These proteins were the products of genes CPR_2403, CPR_0275, CPR_0253, CPR_2284, and CPR_2342 (NCBI Database NC_008262.1). Respectively, these gene products are annotated as putative: elongation factor G, metallo-beta lactamase flavodoxin, peptidyl-prolyl isomerase, electron transfer flavoprotein α chain (EtfA), and butyrate kinase.

Published microarray analyses of stationary phase transcription in *C. acetobutylicum* (46) were analyzed for homologues of the genes identified by our MS analysis. Of the five genes, only CPR_2284 (*etfA*) was shown to be upregulated during the sporulation process. It is thought that EtfA, EtfB, and butyryl-CoA dehydrogenase

(bcd) form a complex that performs the conversion of crotonyl-CoA to butyryl-CoA (17). Due to the genomic arrangement of the genes encoding these three proteins, they had previously been predicted to exist within a single operon (Figure 4.2). The transcriptional analysis of *C. acetobutylicum* indicates that these genes are differentially regulated (46), with EtfA being most strongly expressed during late sporulation, consistent with a potential role in DPA formation.

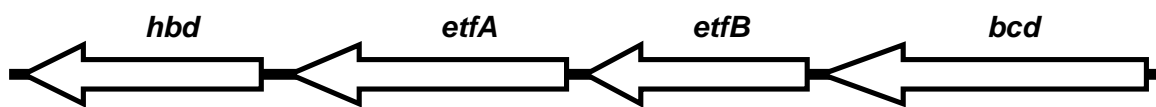


Figure 4.2. Scale representation of the locus containing *etfA*. From right to left the genes are *bcd* encoding butyryl-CoA dehydrogenase, *etfB*, *etfA*, and *hbd* encoding 3-hydroxyl-butryl-CoA dehydrogenase.

Inactivation of *etfA* in *C. perfringens*. Mutant strain Etf1 was constructed by single cross-over insertion of plasmid pSMEtf1 into the *etfA* locus on the chromosome. Etf1 demonstrates no change in vegetative growth, measured as change in optical density at 600 nm (OD_{600}), or in early sporulation, as observed by phase contrast microscopy, relative to the wild-type strain SM101 (data not shown). Sporulating cultures of SM101, Etf1, and the complemented strain Etf2 were analyzed for OD_{600} and DPA content (Figure 4.3). Etf1 produced negligible DPA at all time points, while Etf2 was similar to the wild type strain. These results are similar to the *B. subtilis spoVF* mutant FB106, which has been shown to produce <5% of the wild-type levels of DPA (69).

The *etfA* mutant strain was defective in late stage sporulation (Figure 4.4). Relative numbers of sporulating cells appeared similar during early sporulation of Etf1 and SM101. Phase bright spores within mother cells could be observed in both strains. By eight hours post-inoculation, phase bright SM101 spores were being released by

mother cell lysis, but no phase bright spores were visible in the Etf1 culture. By nine hours post-inoculation, >90% of SM101 visible bodies were phase bright spores that had been released into the medium, while no phase bright spores were evident in the Etf1 culture. The same was true of the Etf1 culture at 24 hours post-inoculation, though the number of cells had dropped by >90%.

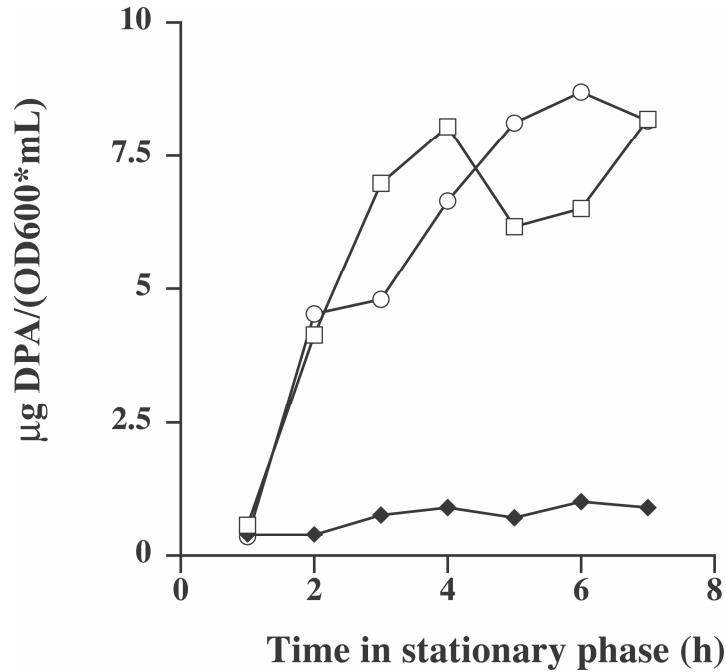


Figure 4.3. Production of DPA by each strain during sporulation. SM101 (wild type) (□), Etf1 (*etfA*⁻) (◆), and Etf2 (*etfA*⁻, pSMnk2/*etfA*⁺) (○) were inoculated into DSSM media. Culture samples were pulled and assayed for OD₆₀₀ and DPA concentration by MRM. The values were adjusted to µg DPA/OD₆₀₀/mL

The effect of *etfA* on spore heat resistance was dramatic. Mature spores in 24 hour cultures of SM101 and Etf2 easily survived the 70°C heat shock necessary to induce efficient germination (38, 43) and then exhibited similar D values at 90°C of 22.1±2.4 and 18.9±2.8, respectively. For Etf1, no viable counts were obtained following the 70°C heat shock alone. *B. subtilis spoVF* mutant strains can take up exogenous DPA and use it to form stable spores (69). However, supplementing Etf1 sporulating culture with

exogenous DPA did not restore spore stability or heat resistance (data not shown). The reason for this is unclear, but a likely explanation is a failure to transport DPA into the mother cell.

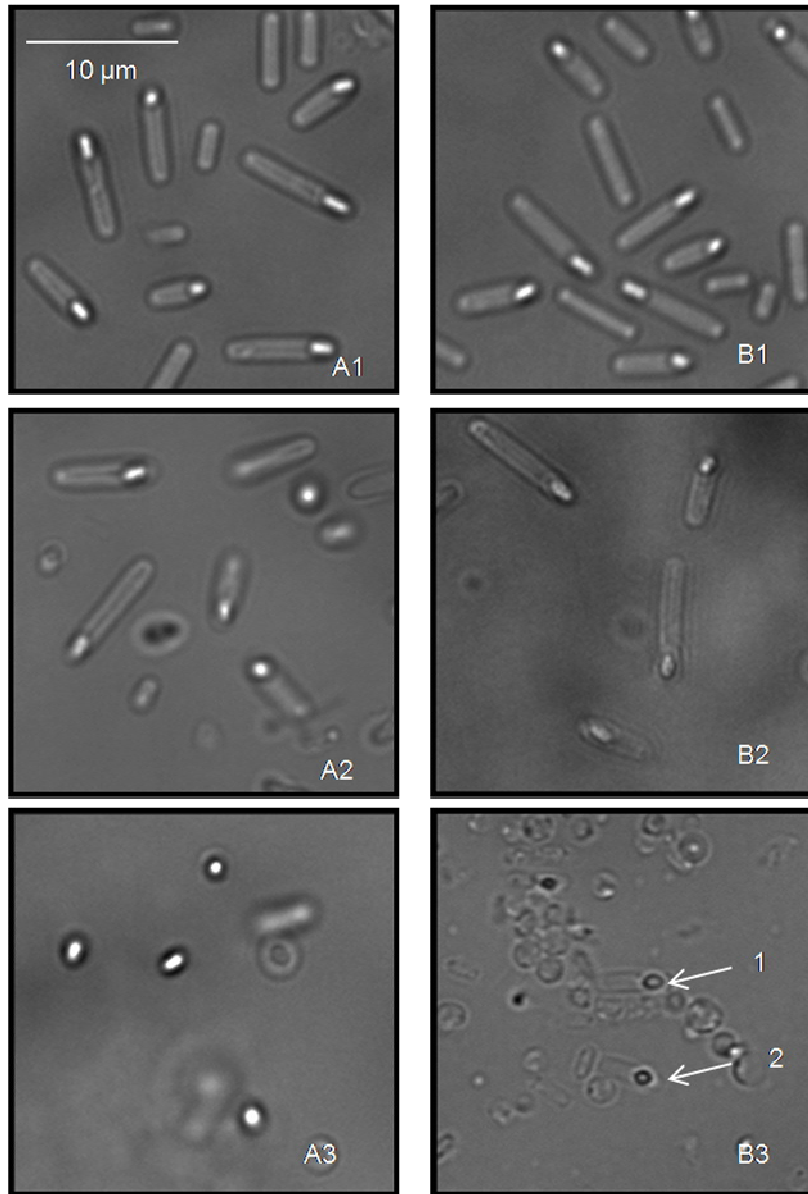


Figure 4.4. Phase contrast images of SM101 and Etf1 during sporulation. SM101 (column A) and Etf1 (column B) were inoculated into DSSM media and sampled for phase contrast microscopy at 6, 8 and 24 hours post inoculation, rows 1, 2, and 3, respectively. The scale for all images match the scale bar in panel A1. Numbers 1 and 2 in panel B3 indicate phase dark spores within partially lysed mother cells.

These observations suggest that Etf1 attempts to produce a stable spore, but the lack of DPA production disrupts the final steps in sporulation. The fact that the endospore initially achieves a phase-bright appearance suggests that other mechanisms allow the endospore to achieve a certain level of dehydration while protected by the mother cell. When the mother cell lyses, it appears that the incomplete spore is incapable of surviving in the surrounding medium.

Recently, a mutant strain of *C. perfringens* was reported with an inactivation of the *spoVA* locus (71). This strain is incapable of transporting DPA that is synthesized in the mother cell into the forespore. Unlike Etf1, the *spoVA* mutant could successfully complete the sporulation process and produce relatively stable spores, but the spores produced were still highly sensitive to heat. The fact that *spoVA* DPA-less spores are stable may result from their loss of a second function of SpoVA in ion release during spore germination (58). The presence of the SpoVA ion channel in the Etf1 DPA-less spores may contribute to their instability.

DPA production by purified DapA and EtfA. To directly demonstrate the roles of DapA and EtfA in our *in vitro* system, we overexpressed and purified the DapA from *C. botulinum* (28) and the EtfA from SM101. The standard *in vitro* assay demonstrated some spontaneous DPA formation in the presence of high concentrations of DapA, as quantified by MRM mass spectrometry (Table 4.2). The same amount of DapA with the addition of EtfA resulted in a 3.4-fold increase in DPA production. EtfA alone, in the absence of DapA, produced no DPA. In order to determine whether spontaneous DPA formation in the absence of EtfA was due to oxidation of the DapA product by dissolved oxygen, the *in vitro* assay was performed simultaneously under aerobic and anoxic

conditions. Under anoxic conditions, spontaneous formation of DPA was reduced by >95%, and addition of EtfA produced a >19-fold increase in DPA synthesis (Table 4.2).

The *in vitro* assay was modified to determine whether a direct interaction of DapA and EtfA was necessary for DPA formation by separating the two proteins with a dialysis membrane within the reaction cell. Following incubation, the reaction resulted in 93% of the level of DPA production in the identical reaction lacking the membrane (Table 4.2 and data not shown). EtfA appears able to act on the product of DapA alone; the reaction does not have to be tied directly to DapA catalysis.

In order to determine if cofactors are involved in the production of DPA, the *in vitro* assay was performed with DapA and EtfA with the addition of NAD, NADP, FAD, or FMN. While NAD did not appear to assist in the reaction, addition of the other three cofactors resulted in an increase in DPA production, with FAD resulting in a nearly 10-fold increase in DPA (data not shown). EtfA contains a putative FAD-binding domain (95). In the absence of added FAD, the purified EtfA protein did not demonstrate an absorbance spectrum characteristic of flavin (83). Following incubation with FAD and repeated washing steps, the protein demonstrated significantly greater absorbance at 280 and 440 nm, characteristic of flavin, than the wash solution (data not shown). The FAD-bound EtfA demonstrated a nearly 3-fold increase in DPA production compared to EtfA washed in the same manner without the addition of FAD (Table 4.2). The production of DPA by EtfA appears to be a catalytic process as each molecule of EtfA is responsible for the production of 67.8 molecules of DPA/minute (data not shown).

Occurrence and function of EtfA. Analysis of the genomes of the sequenced Clostridia revealed multiple homologues of *etfA* in each organism. *C. perfringens* has

two, CPR_2284 (*etfA*) and CPR_0304, which encode products of 335 and 387 amino acids, respectively. The primary difference is that CPR_0304 contains a putative ferredoxin domain at its N-terminal region that is not present in CPR_2284. The sequenced Clostridia all appear to have at least one homologue of both the shorter and the longer *etfA* genes, while many species appear to have multiple copies of one or both. It is unclear what the function of these homologues may be, though to date *etfA* has been implicated in calcium mineralization (11), caffeate respiration (27), butyrate production (89), carnitine reduction (97), and nitrogen fixation (34) in prokaryotes.

In the majority of reactions utilizing EtfA, EtfA is thought to form a heterodimer with the smaller EtfB molecule (83). The structure of the various EtfB molecules has been shown to be highly conserved between organisms. Our results may be the first account of EtfA functioning without an apparent EtfB counterpart.

Table 4.2. Summary of in vitro assays with purified EtfA

Components present in activity assay	DPA produced ($\mu\text{g DPA/mg EtfA/min}$)
DapA aerobic	10.38 ^a
DapA anaerobic	0.012 ^a
DapA + EtfA aerobic	36.52
DapA + EtfA anaerobic	12.36
DapA, EtfA separated by dialysis membrane, aerobic	30.61
DapA + FAD-bound EtfA, aerobic	102.5

^aThese values were calculated as if the reactions contained the same amount of EtfA as that present in the complete reactions.

Proposed function of EtfA in DPA synthesis. Our results demonstrate that EtfA has the ability to catalyze the formation of DPA from the product of the DapA enzyme. The reaction appears to be catalytic, as the amount of EtfA in the activity assay is approximately 0.66 nano mole. Each nano mole of EtfA appears to produce 67 micro mole of DPA per minute in our fastest reaction (data not shown). This activity appears to

occur without direct interaction of the proteins and utilizes FAD as the preferred cofactor. *C. perfringens* EtfA was expressed in *E. coli* cells grown aerobically. It is likely that these cells did not contain enough FAD to saturate the binding domain of the overexpressed EtfA therefore the addition of FAD to the purified protein increased its catalytic activity. The ability of EtfA to convert DHDPA to DPA in the absence of added FAD may be due to the few EtfA molecules that were purified with bound FAD. The percentage of these molecules within the solution of EtfA appears to be very small since we were unable to detect flavin absorbance in our protein sample. The conversion of DHDPA to DPA requires the removal of two hydrogens. We propose that these are passed to the FAD bound to the EtfA molecule, resulting in reduction to FADH₂. The oxidation of FADH₂ to FADH is known to occur spontaneously in the presence of oxygen (42). In our aerobic activity assay, oxygen could easily function as the terminal electron acceptor, as the released electrons would result in H₂O production. This result would explain the 66% reduction in DPA production we observed when the reaction was performed under oxygen-limiting conditions. In the anaerobic conditions under which *C. perfringens* grows, FADH₂ would have to be recycled to FAD by reduction of a protein or cofactor with a higher redox potential, such as rubredoxin, which is known to be present at high concentrations in the cytoplasm (44).

Alternative methods for DPA production. DPA is essential for the formation of stable endospores. The fact that many sporulation-specific genes are highly conserved across all sporeformers, including all clusters of the clostridia as well as the bacilli, indicates that endospore formation was highly developed prior to the divergence of these groups. A survey of 52 species of Firmicutes by PCR amplification of sporulation genes

indicated that *spoVF* is present in the genomes of all spore formers, except for Cluster I clostridia (66), suggesting that this operon was an early component of the sporulation apparatus, but was lost during the evolution of Cluster I. The reason for this is unclear, but it may be due to the presence of a protein or other molecule in the cytoplasm during sporulation that can rapidly oxidize FADH₂. Further work may identify a second molecule essential to DPA production in these organisms.

The Cluster I Clostridia contains at least 25 pathogenic species. Due to the resistance of spores to the conditions of modern sanitation, the spore often plays an essential role in the establishment of the infection. An understanding of DPA production in these organisms may enable blocking of this process, causing loss of spore resistance and breaking the infection cycle.

METHODS

Synthesis of L-ASA. L-ASA was synthesized by the method of Black & Wright (13). Samples were removed throughout the ozonolysis procedure, neutralized with 1N NaHCO₃, and subjected to mass analysis with an ABI-3200 mass spectrometer. The reaction was terminated when the peak corresponding to the deprotonated mass (M-H⁺) of L-allylglycine, 114.1, was completely replaced by the appearance of the peak corresponding to that of L-ASA, 116.1 (data not shown). The functionality of the L-ASA solution was confirmed by the production of DPA by a crude cell extract of a sporulating *B. subtilis* wild type strain. The L-ASA solution was aliquoted and stored at -80°C.

In vitro assay for DPA synthase activity. The system for determining DPA synthase activity was modified from that of Bach & Gilvarg (8). The total reaction volume of 2 mL contained ~3 mg of total protein and 10 mM sodium pyruvate (Fisher) in 20 mM Tris HCl, pH 8.0 and was kept on ice. A freshly thawed tube of L-ASA solution was neutralized with cold 1 M NaHCO₃ and quickly added to the reaction mixture to an approximate concentration of 10 mM. To establish a baseline measurement, 700 μL of the reaction mixture was immediately removed and mixed with 58 μL of 16 M H₂SO₄, vortexed thoroughly, and centrifuged at 13,000 x g for 3 minutes. The remaining reaction mixture was placed in a 37°C water bath for 20 minutes. Following this incubation, 700 μL of the mixture was removed, acidified, and centrifuged in the same manner. The supernatant of both the 'pre' and 'post' reaction samples were extracted with 3 mL diethyl ether. Two 1 mL aliquots of the ether layer were removed. One aliquot was immediately placed into a 1 mL quartz cuvette and the absorbance was determined at 269 nm. The second aliquot was allowed to dry at room temperature

overnight in a fume hood. The sample was then resuspended in 150 μ L 0.01% formic acid, and DPA was quantified by mass spectrometry via multiple reaction monitoring (MRM). In order to assay for the activity of the DPA synthase in the NCTC 8679 protein fractions, the reaction mix contained ~2 mg FB106 (*spoVF::tet*)(69) sporulating crude cell extract as a source of DHDPS or crudely enriched DHDPS from NCTC 8679, in addition to ~2 mg of the NCTC 8679 protein fraction.

The assay was also performed under anoxic conditions in an anaerobic chamber (Coy Labs). The oxygen was allowed to diffuse out of freshly autoclaved water and Tris buffer in the chamber for two days. All reactants were mixed in the chamber with the exception of L-ASA, which was neutralized outside of the chamber, put on ice with the thawed protein samples, and cycled through the airlock. The protein samples and L-ASA were added to the reaction mixture in the chamber and the reaction was performed as described above. The 'pre' and 'post' samples were removed and acidified in the chamber. The samples were removed from the chamber for extraction of DPA.

In order to determine if a direct interaction between DapA and EtfA was necessary for DPA formation *in vitro*, a 1.5 mL reaction mix containing DapA, L-ASA, and pyruvate was placed into a dialysis chamber. Snake Skin dialysis tubing (Thermo-Scientific) with a 3.5 KDa molecular weight cutoff separated this reaction from a 1.5 mL chamber containing only EtfA. Both chambers were buffered with 20mM Tris, pH 8.0. To facilitate the diffusion of molecules across the membrane, the reaction time was lengthened to 45 minutes.

Determination of DPA concentration. DPA was quantified by LC-MS/MS using an ABI 3200 QTrap system in multiple reaction monitoring (MRM) mode. Only

ions with an $M+H^+$ of 168.1 ± 0.2 that produced daughter ions with an $M+H^+$ of 127.1 ± 0.2 were used for quantization. A standard curve was developed using pure DPA extracted in ether as described above (Sigma).

Enrichment of the DPA synthase from NCTC 8679. 0.5 L cultures of sporulating cells were harvested at 11.5 hours post-inoculation, centrifuged for 15 min at 4°C at $6,000 \times g$, washed twice with cold deionized water, and resuspended in 50 mL cold 20 mM Tris, pH 8.0. The cells were then ruptured by sonication on ice, and the suspension was centrifuged at $60,000 \times g$ for 30 min. The supernatant was collected to obtain the crude cell extract. This extract was fractionated by successive precipitation with ammonium sulfate ($(\text{NH}_4)_2\text{SO}_4$) at concentrations of: 20%, 40%, 55%, 70% and 80% saturation at 4°C . The fractions were desalted by dialysis and assayed for DPA synthase activity by the *in vitro* assay with DHDPS provided by the FB106 crude cell extract.

The 55-70% fraction was separated into five fractions by cation exchange chromatography with a 1 mL HiTrap QXL column. These fractions were assayed by the *in vitro* assay with the 40-55% $(\text{NH}_4)_2\text{SO}_4$ fraction serving as the source of DHDPS. The active fraction was desalted with a HiTrap Desalting column and separated by size exclusion chromatography on a 120 mL 1.6 cm by 60 cm Superdex 200 column (GE Healthcare).

Native-PAGE assays for DPA synthase activity. The active fraction collected from size exclusion chromatography was concentrated 10-fold by use of a Centricon filtration device (Millipore) with a 10 kDa cutoff. The fraction was then separated by native-PAGE with an 8% acrylamide gel at 4°C . After electrophoresis, the gel was

briefly washed in cold 20mM Tris, pH 8.0 to remove the glycine from the PAGE buffer. The gel was then cut down the center with a razor blade. One half was rapidly stained with Coomassie brilliant blue. The other half of the gel was placed on a glass plate over a grid and 2 mm sections of the lane containing the active fraction were excised. The stained gel as well as the prestained marker served as guides for the excision process. One mm sections were cut off of each end of each gel slice and immediately stored at -80°C. The remainder of each gel slice was placed into the *in vitro* activity assay. The reaction was allowed to proceed for 30 min to facilitate the diffusion of the reactants into, and the products out of, the gel slice. The adjacent two gel slices that were found to have activity were removed from the reaction mixture, washed twice with 20 mM Tris, pH 8.0 and were stored at -80°C. One half of each slice was removed for analysis by SDS-PAGE, the other half as well as the gel fragments removed prior to the assay were prepared for peptide identification. In-gel trypsin digestion was performed (45), and the peptides were analyzed using an ABI-4800 MalDI-TOF/TOF. The peptide fragmentation data was analyzed with MASCOT (Matrix Science) using the NCBI nr database.

Construction of mutant strains. The construction of mutant and complemented strains in SM101 has been previously described (65, 68). Briefly, primers Mnk3 and Mnk4 were used to PCR amplify a 500 bp internal region of *etfA*. This product was ligated into pSM300 to form pSMnk1. SM101 was transformed by electroporation with pSMnk1, and strain Etf1 was selected by growth on BHI with 30 µg/mL erythromycin. Insertion of pSMnk1 into *etfA* was verified by PCR using primers Mnk5 and OSM214. To complement *etfA*, primers Mnk8 and Mnk9 were used to PCR amplify *etfA* plus the upstream 150 bp. This product was ligated into pJIR750 to form pJIRMnk2, which was

electroporated into Etf1. A successful transformant, Etf2, was identified by growth on BHI containing 30 µg/ mL erythromycin and 20 µg/mL chloramphenicol.

Table 4.3. Primers and used in this study

Primer	Primer Sequence
Mnk7	GCGTTAACAAAGTGGTTTAATTAAGGGAGGTATTTAAGATGAATAAGC
Mnk8	CTCAGGATCCAAGCTTGC GGCCGCTATTCCAGCACCCATTGTACCTGC
Mnk9	GCTTGTCGACGGTTAAAAGGATCTCCACAAAG
Mnk10	CGAAGGATCCTGGGAGGTATTTAAGATG
Mnk11	GATGCGGCCGCTTAAGCTTCTTCCTCCTTCATAGCTTTT
Mnk12	GATGGGGCCGCAGCTTCTTCCTTCATAGC
OSM215	GTTATTA ACTATTTATCAATTCCTGCA

Table 4.4. Strains used in this study.

Name	Description	Reference
NCTC 8679	<i>C. perfringens</i> food poisoning isolate	(67)
SM101	<i>C. perfringens</i> NCTC 8798, electroporatable	(107)
FB106	<i>spoVF::Tet</i> in <i>B. subtilis</i> PS832 background	(69)
Mnk1	SM101, <i>etfA::erm</i>	This study
Mnk2	SM101, <i>etfA::erm</i> , pJMnk1:: <i>Cm</i>	This study
BL21-CodonPlus-RIL	<i>E. coli</i> overexpression strain pLysS:: <i>Cm</i>	Stratagene

Purification of DapA and EtfA. The overexpression of *C. botulinum* DapA was achieved by use of pETSA1, which was a gift from Renwick Dobson, and purification of this protein was performed as previously described (3, 28). The SM101 *etfA* was amplified with primers Mnk10 and Mnk11 and was ligated between the BamHI and NotI sites of pET21a (Novagen) in frame with an N-terminal T7 tag and a C-terminal histidine tag. The resulting plasmid, pETFa2 was transformed into BL21-CodonPlus-RIL *E. coli* (Stratagene). The cells were grown to an OD₆₀₀ of 0.8 and induced with 1mM IPTG for 3 hours. Cells were pelleted at 4,000 x g for 20 min, resuspended in lysis buffer containing 30 mM imidazole and 20 mM Tris-HCl, pH 8.0 and lysed by sonication on ice. The lysate was centrifuged at 50,000 x g for 30 min and the supernatant was retained as the

crude cell extract. The extract was passed over a 5 mL His Trap FF Column (GE Healthcare) and washed with 20 mL lysis buffer. The His-tagged EtfA was obtained by elution with 300 mM imidazole, 20 mM Tris, pH 8.0. The imidazole was removed by dialysis against 20 mM Tris, with three changes of buffer over 24 hours. The purity of EtfA and DapA were confirmed by SDS-PAGE.

ACKNOWLEDGEMENTS

This project was supported by the National Research Initiative of the USDA Cooperative State Research, Education and Extension Service, grant number 2004-04069, and by a Virginia Tech 2010 Ph.D. Fellowship Program. We thank Matt Perugini and Renwick Dobson for the DapA overexpression vector and Keith Ray of the Virginia Tech Mass Spectrometry incubator for assistance in protein identification.

Chapter 5

Final Discussion

Bacterial spores play a key role in the establishment of diseases caused by sporulating bacteria. Despite the advances in modern sanitation of the last century, the natural resistance properties of the spore allow it to survive treatments that would kill any other cell type. For this reason, a tremendous amount of research has been performed studying these cells, particularly the spores produced by the bacilli. From this research the sporulation process has emerged as the most complete model of cellular differentiation (Reviewed in, (30). Despite the volume of effort devoted to sporulation research as a whole, relatively little work has been performed on the spores and sporulation process of the clostridia, a genus that includes no less than 16 known pathogenic species (23). The work that has been done has been sporadic throughout the literature as no model organism for clostridial sporulation has been universally accepted. The genus clostridia is widely regarded as one of the most diverse of all bacterial groupings, with the origins of many species thought to date back more than 2.7 billion years ago, predating the 'oxygen catastrophe' of the early Paleoproterozoic era. The tremendous diversity within this ancient genus makes selection of a true model organism a difficult task (72).

As one of the most widely occurring bacterial pathogens, the study of the spores and sporulation of *C. perfringens* would appear an obvious choice for concentrated effort. The heat resistance of *C. perfringens* spores has been addressed recently by several studies, with work focused on determining why CPE+ strains produce spores that are more resistant to heat than the spores produced by other strains (55, 64, 81). The research presented in this dissertation is focused on this question, as well as on

understanding how *C. perfringens* produces DPA, a compound that is essential for spore resistance to wet heat and UV radiation.

In Chapter 2, we detail our study of the spores produced by 5 CPE+ and 4 CPE- strains. These spores were analyzed for properties that have been shown to be linked to heat resistance in other species, such as core density and solute contents and cortex structure (12, 76). In characterizing the spore peptidoglycan, we observed that *C. perfringens* possesses a novel cortex structure. Unlike the spores of organisms previously studied, all *C. perfringens* strains lack the single L-alanine residues present on nearly 50% of the unmodified muramic acid residues of other species (74). The peptidoglycan also appears to have a higher degree of de-*N*-acetylation than other organisms (6). Although it appears that the general peptidoglycan structure is shared between *C. perfringens* strains, we observed that CPE+ strains demonstrated a higher ratio of cortex to germ cell wall than CPE- strains. In Chapter 3, we detail the construction of a *dacF* mutant strain of CPE+ strain SM101. This strain appears to produce spores exhibiting a lower ratio of cortex to germ cell wall than the wild type strain, with a corresponding decrease in spore heat resistance. From these results we conclude that the ratio of germ cell wall to cortex is an important determinant of heat resistance in *C. perfringens*.

In order to determine the peptidoglycan structure of these strains, we used LC-MS/MS for the elucidation of muropeptides structure. This procedure was considerably faster than previously employed methods (9, 75). Although we collected muropeptides and identified them individually, it is likely that optimization of buffer conditions for

separation with MS-compatible compounds could lead to the elucidation of a complete peptidoglycan structure in a single experiment.

The other features analyzed in our wild-type strains did more to highlight the diversity present in this species than to provide clear links to heat resistance. The most heat resistant spores were shown to possess the smallest, most dehydrated spore cores. The least heat resistant spores studied were produced by Strain 13. While these spores possessed the least dense, most hydrated spore cores, the values obtained for the spores of other strains did not follow a clear trend. We conclude that a minimum degree of spore core dehydration must be met to form a stable spore. Once this value is met, however, the contribution of other factors is more important to spore heat resistance. In Chapter 3, we describe a mutant strain of SM101 with an inactivated *spmA/B* locus. This strain produces spores which can not achieve the dehydration levels of spores formed by Strain 13. These spores are dramatically less heat resistant than wild-type spores and demonstrate a measurable death curve at both room and refrigeration temperatures, supporting our original conclusion.

These results show that there are clear differences between the most and least heat resistant spores. Outside of these extreme examples we concluded that other unknown, factors must be responsible for the difference in heat resistance between strains. In 2008 Li & McClane identified a protein, Ssp4, which appeared to be directly linked to heat resistance. This study revealed that CPE- strains exhibited one form of this protein, while CPE+ strains expressed a variant protein with a single amino acid substitution. Replacement of the Ssp4 of a CPE+ strain with the protein from a CPE- strain dramatically reduced spore heat resistance, but not to the levels of the CPE- strain the

protein came from (56). Ssp4 may be one factor that determines the heat resistance of the spores that fell between the most and least heat resistant strains.

DPA is a major component of all known bacterial spores and is produced in *B. subtilis* during late stage sporulation by the products of the *spoVF* operon (21, 25, 69). Reduction of DPA content by chemical or genetic methods results in spores that are significantly less resistant to wet heat and UV radiation. All studied members of the Cluster I clostridia lack *spoVF*, but produce DPA (66, 72). In Chapter 4, we detail our search for the DPA synthase of *C. perfringens*. We determined that the product of the *etfA* gene is responsible for converting DHDPA to DPA by aiding in the transfer of two electrons and two protons from DHDPA to FAD. In our *in vitro* assay FADH₂ is recycled by spontaneous oxidation in air. It is unclear what would serve as the electron acceptor in the cytoplasm of sporulating *C. perfringens*, but it is likely that another protein or molecule capable of rapidly oxidizing FADH₂ is present in *C. perfringens* that is essential for DPA production *in vivo*.

The spores of *C. perfringens* are responsible for nearly 240,000 cases of food poisoning each year in the U.S. as well as approximately 140 deaths per year from gas gangrene (61). Understanding how these spores are made as well as how they achieve their remarkable resistance to heat and UV radiation may allow the development of methods to decrease the incidence of these diseases. Beyond this obvious application, it must be recognized that this knowledge may also assist in the reduction of diseases caused by other clostridia, particularly the members of Cluster I, which include the deadly pathogens *C. botulinum* and *C. tetani*.

REFERENCES

1. **Alsaker, K. V., and E. T. Papoutsakis.** 2005. Transcriptional program of early sporulation and stationary-phase events in *Clostridium acetobutylicum*. *J Bacteriol* **187**:7103-18.
2. **Ando, Y., T. Tsuzuki, H. Sunagawa, and S. Oka.** 1985. Heat resistance, spore germination, and enterotoxigenicity of *Clostridium perfringens*. *Microbiol Immunol* **29**:317-326.
3. **Atkinson, S. C., R. C. Dobson, J. M. Newman, M. A. Gorman, C. Dogovski, M. W. Parker, and M. A. Perugini.** 2009. Crystallization and preliminary X-ray analysis of dihydrodipicolinate synthase from *Clostridium botulinum* in the presence of its substrate pyruvate. *Acta Crystallogr Sect F Struct Biol Cryst Commun* **65**:253-5.
4. **Atrih, A., G. Bacher, G. Allmaier, M. P. Williamson, and S. J. Foster.** 1999. Analysis of peptidoglycan structure from vegetative cells of *Bacillus subtilis* 168 and role of PBP 5 in peptidoglycan maturation. *J Bacteriol* **181**:3956-3966.
5. **Atrih, A., G. Bacher, R. Korner, G. Allmaier, and S. J. Foster.** 1999. Structural analysis of *Bacillus megaterium* KM spore peptidoglycan and its dynamics during germination. *Microbiology* **145** (Pt 5):1033-1041.
6. **Atrih, A., and S. J. Foster.** 2001. Analysis of the role of bacterial endospore cortex structure in resistance properties and demonstration of its conservation amongst species. *J Appl Microbiol* **91**:364-372.
7. **Atrih, A., and S. J. Foster.** 1999. The role of peptidoglycan structure and structural dynamics during endospore dormancy and germination. *Antonie Van Leeuwenhoek* **75**:299-307.
8. **Bach, M. L., and C. Gilvarg.** 1966. Biosynthesis of dipicolinic acid in sporulating *Bacillus megaterium*. *J Biol Chem* **241**:4563-4.
9. **Bacher, G., R. Korner, A. Atrih, S. J. Foster, P. Roepstorff, and G. Allmaier.** 2001. Negative and positive ion matrix-assisted laser desorption/ionization time-of-flight mass spectrometry and positive ion nano-electrospray ionization quadrupole ion trap mass spectrometry of peptidoglycan fragments isolated from various *Bacillus* species. *J Mass Spectrom* **36**:124-139.
10. **Balassa, G., P. Milhaud, E. Raulet, M. T. Silva, and J. C. Sousa.** 1979. A *Bacillus subtilis* mutant requiring dipicolinic acid for the development of heat-resistant spores. *J Gen Microbiol* **110**:365-79.
11. **Barabesi, C., A. Galizzi, G. Mastromei, M. Rossi, E. Tamburini, and B. Perito.** 2007. *Bacillus subtilis* gene cluster involved in calcium carbonate biomineralization. *J Bacteriol* **189**:228-35.
12. **Beaman, T. C., J. T. Greenamyre, T. R. Corner, H. S. Pankratz, and P. Gerhardt.** 1982. Bacterial spore heat resistance correlated with water content, wet density, and protoplast/sporoplast volume ratio. *J Bacteriol* **150**:870-877.
13. **Black, S., and N. G. Wright.** 1955. Beta-Aspartokinase and Beta-aspartyl phosphate. *J Biol Chem* **213**:27-38.
14. **Boland, F. M., A. Atrih, H. Chirakkal, S. J. Foster, and A. Moir.** 2000. Complete spore-cortex hydrolysis during germination of *Bacillus subtilis* 168 requires SleB and YpeB. *Microbiology* **146** (Pt 1):57-64.

15. **Borriello, S. P.** 1995. *Clostridial* disease of the gut. *Clin Infect Dis* **20 Suppl 2**:S242-250.
16. **Boughton, B. A., R. C. Dobson, J. A. Gerrard, and C. A. Hutton.** 2008. Conformationally constrained diketopimelic acid analogues as inhibitors of dihydrodipicolinate synthase. *Bioorg Med Chem Lett* **18**:460-3.
17. **Boynton, Z. L., G. N. Bennet, and F. B. Rudolph.** 1996. Cloning, sequencing, and expression of clustered genes encoding beta-hydroxybutyryl-coenzyme A (CoA) dehydrogenase, crotonase, and butyryl-CoA dehydrogenase from *Clostridium acetobutylicum* ATCC 824. *J Bacteriol* **178**:3015-24.
18. **Brynstad, S., M. R. Sarker, B. A. McClane, P. E. Granum, and J. I. Rood.** 2001. Enterotoxin plasmid from *Clostridium perfringens* is conjugative. *Infect Immun* **69**:3483-3487.
19. **Buchanan, C. E., and M. L. Ling.** 1992. Isolation and sequence analysis of *dacB*, which encodes a sporulation-specific penicillin-binding protein in *Bacillus subtilis*. *J Bacteriol* **174**:1717-25.
20. **Bukhari, A. I., and A. L. Taylor.** 1971. Genetic analysis of diaminopimelic acid- and lysine-requiring mutants of *Escherichia coli*. *J Bacteriol* **105**:844-54.
21. **Chen, N. Y., S. Q. Jiang, D. A. Klein, and H. Paulus.** 1993. Organization and nucleotide sequence of the *Bacillus subtilis* diaminopimelate operon, a cluster of genes encoding the first three enzymes of diaminopimelate synthesis and dipicolinate synthase. *J Biol Chem* **268**:9448-65.
22. **Church, B. D., and H. Halvorson.** 1959. Dependence of the heat resistance of bacterial endospores on their dipicolinic acid content. *Nature* **183**:124-125.
23. **Clarke, N. M. D. (ed.).** 1989. *Clostridia*, 1 ed, vol. 3. Plenum Press, New York.
24. **Collie, R. E., and B. A. McClane.** 1998. Evidence that the enterotoxin gene can be episomal in *Clostridium perfringens* isolates associated with non-food-borne human gastrointestinal diseases. *J Clin Microbiol* **36**:30-36.
25. **Daniel, R. A., and J. Errington.** 1993. Cloning, DNA sequence, functional analysis and transcriptional regulation of the genes encoding dipicolinic acid synthetase required for sporulation in *Bacillus subtilis*. *J Mol Biol* **232**:468-83.
26. **Daube, G., P. Simon, B. Limbourg, C. Manteca, J. Mainil, and A. Kaeckenbeek.** 1996. Hybridization of 2,659 *Clostridium perfringens* isolates with gene probes for seven toxins (alpha, beta, epsilon, iota, theta, mu, and enterotoxin) and for sialidase. *Am J Vet Res* **57**:496-501.
27. **Dilling, S., F. Imkamp, S. Schmidt, and V. Muller.** 2007. Regulation of caffeate respiration in the acetogenic bacterium *Acetobacterium woodii*. *Appl Environ Microbiol* **73**:3630-6.
28. **Dobson, R. C., S. C. Atkinson, M. A. Gorman, J. M. Newman, M. W. Parker, and M. A. Perugini.** 2008. The purification, crystallization and preliminary X-ray diffraction analysis of dihydrodipicolinate synthase from *Clostridium botulinum*. *Acta Crystallogr Sect F Struct Biol Cryst Commun* **64**:206-8.
29. **Dowd, M. M., B. Orsburn, and D. L. Popham.** 2008. Cortex peptidoglycan lytic activity in germinating *Bacillus anthracis* spores. *J Bacteriol* **190**:4541-8.
30. **Driks, A.** 1999. *Bacillus subtilis* spore coat. *Microbiol Mol Biol Rev* **63**:1-20.
31. **Driks, A.** 2002. Overview: Development in bacteria: spore formation in *Bacillus subtilis*. *Cell Mol Life Sci* **59**:389-91.

32. **Duncan, C. L., and D. H. Strong.** 1968. Improved medium for sporulation of *Clostridium perfringens*. *Appl Microbiol* **16**:82-89.
33. **Duncan, C. L., H. Sugiyama, and D. H. Strong.** 1968. Rabbit ileal loop response to strains of *Clostridium perfringens*. *J Bacteriol* **95**:1560-1566.
34. **Earl, C. D., C. W. Ronson, and F. M. Ausubel.** 1987. Genetic and structural analysis of the *Rhizobium meliloti fixA, fixB, fixC, and fixX* genes. *J Bacteriol* **169**:1127-36.
35. **Errington, J.** 2003. Regulation of endospore formation in *Bacillus subtilis*. *Nat Rev Microbiol* **1**:117-26.
36. **Fukuda, A., and C. Gilvarg.** 1968. The relationship of dipicolinate and lysine biosynthesis in *Bacillus megaterium*. *J Biol Chem* **243**:3871-6.
37. **Hall, H. E., R. Angelotti, K. H. Lewis, and M. J. Foter.** 1963. Characteristics of *Clostridium perfringens* Strains Associated with Food and Food-Borne Disease. *J Bacteriol* **85**:1094-1103.
38. **Harry, K. H., R. Zhou, L. Kroos, and S. B. Melville.** 2009. Sporulation and enterotoxin (CPE) synthesis are controlled by the sporulation-specific sigma factors SigE and SigK in *Clostridium perfringens*. *J Bacteriol*.
39. **Helmann, J. D. M., C.P., Jr.** 2002. RNA polymerase and sigma factors, p. 289-312. *In* J. A. H. A.L. Sonenshein, R. Losick (ed.), *Bacillus subtilis* and Its Closest Relatives: From Genes to Cells. American Society for Microbiology, Washington D.C.
40. **Henriques, A. O., L. R. Melsen, and C. P. Moran, Jr.** 1998. Involvement of superoxide dismutase in spore coat assembly in *Bacillus subtilis*. *J Bacteriol* **180**:2285-91.
41. **Horsburgh, G. J., A. Atrih, and S. J. Foster.** 2003. Characterization of LytH, a differentiation-associated peptidoglycan hydrolase of *Bacillus subtilis* involved in endospore cortex maturation. *J Bacteriol* **185**:3813-3820.
42. **Iyanagi, T., N. Makino, and H. S. Mason.** 1974. Redox properties of the reduced nicotinamide adenine dinucleotide phosphate-cytochrome P-450 and reduced nicotinamide adenine dinucleotide-cytochrome b5 reductases. *Biochemistry* **13**:1701-10.
43. **Janssen, F. W., A. J. Lund, and L. E. Anderson.** 1958. Colorimetric assay for dipicolinic acid in bacterial spores. *Science* **127**:26-27.
44. **Jean, D., V. Briolat, and G. Reysset.** 2004. Oxidative stress response in *Clostridium perfringens*. *Microbiology* **150**:1649-59.
45. **Jeno, P., T. Mini, S. Moes, E. Hintermann, and M. Horst.** 1995. Internal sequences from proteins digested in polyacrylamide gels. *Anal Biochem* **224**:75-82.
46. **Jones, S. W., C. J. Paredes, B. Tracy, N. Cheng, R. Sillers, R. S. Senger, and E. T. Papoutsakis.** 2008. The transcriptional program underlying the physiology of *Clostridial* sporulation. *Genome Biol* **9**:R114.
47. **Kihm, D. J., M. T. Hutton, J. H. Hanlin, and E. A. Johnson.** 1990. Influence of transition metals added during sporulation on heat resistance of *Clostridium botulinum* 113B spores. *Appl Environ Microbiol* **56**:681-685.

48. **Kimura, K.** 1974. Pyridine-2,6-dicarboxylic acid (dipicolinic acid) formation in *Bacillus subtilis*. I. Non-enzymatic formation of dipicolinic acid from pyruvate and aspartic semialdehyde. *J Biochem* **75**:961-7.
49. **Kimura, K., and T. Sasakawa.** 1975. Pyridine-2, 6-dicarboxylic acid (dipicolinic acid) formation in *Bacillus subtilis*. II Non-enzymatic and enzymatic formations of dipicolinic acid from alpha, epsilon-diketopimelic acid and ammonia. *J Biochem* **78**:381-90.
50. **Kobayashi, K., S. D. Ehrlich, A. Albertini, G. Amati, K. K. Andersen, M. Arnaud, K. Asai, S. Ashikaga, S. Aymerich, P. Bessieres, F. Boland, S. C. Brignell, S. Bron, K. Bunai, J. Chapuis, L. C. Christiansen, A. Danchin, M. Debarbouille, E. Dervyn, E. Deuerling, K. Devine, S. K. Devine, O. Dreesen, J. Errington, S. Fillinger, S. J. Foster, Y. Fujita, A. Galizzi, R. Gardan, C. Eschevins, T. Fukushima, K. Haga, C. R. Harwood, M. Hecker, D. Hosoya, M. F. Hullo, H. Kakeshita, D. Karamata, Y. Kasahara, F. Kawamura, K. Koga, P. Koski, R. Kuwana, D. Imamura, M. Ishimaru, S. Ishikawa, I. Ishio, D. Le Coq, A. Masson, C. Mauel, R. Meima, R. P. Mellado, A. Moir, S. Moriya, E. Nagakawa, H. Nanamiya, S. Nakai, P. Nygaard, M. Ogura, T. Ohanan, M. O'Reilly, M. O'Rourke, Z. Pragai, H. M. Pooley, G. Rapoport, J. P. Rawlins, L. A. Rivas, C. Rivolta, A. Sadaie, Y. Sadaie, M. Sarvas, T. Sato, H. H. Saxild, E. Scanlan, W. Schumann, J. F. Seegers, J. Sekiguchi, A. Sekowska, S. J. Seror, M. Simon, P. Stragier, R. Studer, H. Takamatsu, T. Tanaka, M. Takeuchi, H. B. Thomaidis, V. Vagner, J. M. van Dijl, K. Watabe, A. Wipat, H. Yamamoto, M. Yamamoto, Y. Yamamoto, K. Yamane, K. Yata, K. Yoshida, H. Yoshikawa, U. Zuber, and N. Ogasawara.** 2003. Essential *Bacillus subtilis* genes. *Proc Natl Acad Sci U S A* **100**:4678-83.
51. **Kokai-Kun, J. F., J. G. Songer, J. R. Czczulin, F. Chen, and B. A. McClane.** 1994. Comparison of Western immunoblots and gene detection assays for identification of potentially enterotoxigenic isolates of *Clostridium perfringens*. *J Clin Microbiol* **32**:2533-2539.
52. **Kozuka, S., and K. Tochikubo.** 1983. Triple fixation of *Bacillus subtilis* dormant spores. *J Bacteriol* **156**:409-413.
53. **Labbe, R. G.** 1981. Enterotoxin formation by *Clostridium perfringens* type A in a defined medium. *Appl Environ Microbiol* **41**:315-317.
54. **Le Blanc, J. C., J. W. Hager, A. M. Ilisiu, C. Hunter, F. Zhong, and I. Chu.** 2003. Unique scanning capabilities of a new hybrid linear ion trap mass spectrometer (Q TRAP) used for high sensitivity proteomics applications. *Proteomics* **3**:859-869.
55. **Li, J., and B. A. McClane.** 2006. Further comparison of temperature effects on growth and survival of *Clostridium perfringens* type A isolates carrying a chromosomal or plasmid-borne enterotoxin gene. *Appl Environ Microbiol* **72**:4561-4568.
56. **Li, J., and B. A. McClane.** 2008. A novel small acid soluble protein variant is important for spore resistance of most *Clostridium perfringens* food poisoning isolates. *PLoS Pathog* **4**:e1000056.

57. **Lindsay, J. A., T. C. Beaman, and P. Gerhardt.** 1985. Protoplast water content of bacterial spores determined by buoyant density sedimentation. *J Bacteriol* **163**:735-737.
58. **Magge, A., A. C. Granger, P. G. Wahome, B. Setlow, V. R. Vepachedu, C. A. Loshon, L. Peng, D. Chen, Y. Q. Li, and P. Setlow.** 2008. Role of dipicolinic acid in the germination, stability, and viability of spores of *Bacillus subtilis*. *J Bacteriol* **190**:4798-807.
59. **Martin, H. H., and J. W. Foster.** 1958. Biosynthesis of dipicolinic acid in *Bacillus megaterium*. *J Bacteriol* **76**:167-78.
60. **McClane, B. A.** 2005. *Clostridial* Enterotoxins, p. 385-406. In P. Durre (ed.), *Handbook on Clostridia*. Taylor & Francis Group, Boca Raton, FL.
61. **Mead, P. S., L. Slutsker, P. M. Griffin, and R. V. Tauxe.** 1999. Food-related illness and death in the United States. *Emerg Infect Dis* **5**:841-842.
62. **Meador-Parton, J., and D. L. Popham.** 2000. Structural analysis of *Bacillus subtilis* spore peptidoglycan during sporulation. *J Bacteriol* **182**:4491-4499.
63. **Nicholson, W. S., Peter.** 1990. Sporulation, Germination and Outgrowth. In C. R. C. Harwood, S.M. (ed.), *Molecular Methods for Bacillus*. John Wiley & Sons, West Sussex.
64. **Novak, J. S., V. K. Juneja, and B. A. McClane.** 2003. An ultrastructural comparison of spores from various strains of *Clostridium perfringens* and correlations with heat resistance parameters. *Int J Food Microbiol* **86**:239-247.
65. **O'Brien, D. K., and S. B. Melville.** 2004. Effects of *Clostridium perfringens* alpha-toxin (PLC) and perfringolysin O (PFO) on cytotoxicity to macrophages, on escape from the phagosomes of macrophages, and on persistence of *C. perfringens* in host tissues. *Infect Immun* **72**:5204-15.
66. **Onyenwoke, R. U., J. A. Brill, K. Farahi, and J. Wiegel.** 2004. Sporulation genes in members of the low G+C Gram-type-positive phylogenetic branch (*Firmicutes*). *Arch Microbiol* **182**:182-92.
67. **Orsburn, B., S. B. Melville, and D. L. Popham.** 2008. Factors contributing to heat resistance of *Clostridium perfringens* endospores. *Appl Environ Microbiol* **74**:3328-35.
68. **Orsburn, B., K. Sucre, D. L. Popham, and S. B. Melville.** 2009. The SpmA/B and DacF proteins of *Clostridium perfringens* play important roles in spore heat resistance. *FEMS Microbiol Lett* **291**:188-94.
69. **Paidhungat, M., B. Setlow, A. Driks, and P. Setlow.** 2000. Characterization of spores of *Bacillus subtilis* which lack dipicolinic acid. *J Bacteriol* **182**:5505-5012.
70. **Paredes-Sabja, D., N. Sarker, B. Setlow, P. Setlow, and M. R. Sarker.** 2008. Roles of DacB and Spm proteins in *Clostridium perfringens* spore resistance to moist heat, chemicals and UV radiation. *Appl Environ Microbiol*.
71. **Paredes-Sabja, D., B. Setlow, P. Setlow, and M. R. Sarker.** 2008. Characterization of *Clostridium perfringens* spores that lack SpoVA proteins and dipicolinic acid. *J Bacteriol* **190**:4648-59.
72. **Paredes, C. J., K. V. Alsaker, and E. T. Papoutsakis.** 2005. A comparative genomic view of *Clostridial* sporulation and physiology. *Nat Rev Microbiol* **3**:969-78.

73. **Popham, D. L., M. E. Gilmore, and P. Setlow.** 1999. Roles of low-molecular-weight penicillin-binding proteins in *Bacillus subtilis* spore peptidoglycan synthesis and spore properties. *J Bacteriol* **181**:126-132.
74. **Popham, D. L., J. Helin, C. E. Costello, and P. Setlow.** 1996. Analysis of the peptidoglycan structure of *Bacillus subtilis* endospores. *J Bacteriol* **178**:6451-6458.
75. **Popham, D. L., J. Helin, C. E. Costello, and P. Setlow.** 1996. Muramic lactam in peptidoglycan of *Bacillus subtilis* spores is required for spore outgrowth but not for spore dehydration or heat resistance. *Proc Natl Acad Sci U S A* **93**:15405-15410.
76. **Popham, D. L., B. Illades-Aguilar, and P. Setlow.** 1995. The *Bacillus subtilis* *dacB* gene, encoding penicillin-binding protein 5*, is part of a three-gene operon required for proper spore cortex synthesis and spore core dehydration. *J Bacteriol* **177**:4721-4729.
77. **Raju, D., and M. R. Sarker.** 2005. Comparison of the levels of heat resistance of wild-type, *cpe* knockout, and *cpe* plasmid-cured *Clostridium perfringens* type A strains. *Appl Environ Microbiol* **71**:7618-7620.
78. **Raju, D., M. Waters, P. Setlow, and M. R. Sarker.** 2006. Investigating the role of small, acid-soluble spore proteins (SASPs) in the resistance of *Clostridium perfringens* spores to heat. *BMC Microbiol* **6**:50.
79. **Rohrs, B.** *Clostridium perfringens*, Not the 24 hour flu. In *F. a. C. Sciences* (ed.), Columbus, Ohio.
80. **Sacks, L. E., and P. A. Thompson.** 1978. Clear, defined medium for the sporulation of *Clostridium perfringens*. *Appl Environ Microbiol* **35**:405-410.
81. **Sarker, M. R., R. P. Shivers, S. G. Sparks, V. K. Juneja, and B. A. McClane.** 2000. Comparative experiments to examine the effects of heating on vegetative cells and spores of *Clostridium perfringens* isolates carrying plasmid genes versus chromosomal enterotoxin genes. *Appl Environ Microbiol* **66**:3234-3240.
82. **Sarker, M. R., R. P. Shivers, S. G. Sparks, V. K. Juneja, and B. A. McClane.** 2000. Comparative experiments to examine the effects of heating on vegetative cells and spores of *Clostridium perfringens* isolates carrying plasmid genes versus chromosomal enterotoxin genes. *Appl Environ Microbiol* **66**:3234-40.
83. **Sato, K., Y. Nishina, and K. Shiga.** 2003. Purification of electron-transferring flavoprotein from *Megasphaera elsdenii* and binding of additional FAD with an unusual absorption spectrum. *J Biochem* **134**:719-29.
84. **Setlow, B., and P. Setlow.** 1993. Dipicolinic Acid Greatly Enhances Production of Spore Photoproduct in Bacterial Spores upon UV Irradiation. *Appl Environ Microbiol* **59**:640-643.
85. **Setlow, P.** 2003. Spore germination. *Curr Opin Microbiol* **6**:550-6.
86. **Setlow, P.** 2006. Spores of *Bacillus subtilis*: their resistance to and killing by radiation, heat and chemicals. *J Appl Microbiol* **101**:514-525.
87. **Shih, N. J., and R. G. Labbe.** 1996. Sporulation-promoting ability of *Clostridium perfringens* culture fluids. *Appl Environ Microbiol* **62**:1441-1443.
88. **Shimizu, T., K. Ohtani, H. Hirakawa, K. Ohshima, A. Yamashita, T. Shiba, N. Ogasawara, M. Hattori, S. Kuhara, and H. Hayashi.** 2002. Complete

- genome sequence of *Clostridium perfringens*, an anaerobic flesh-eater. Proc Natl Acad Sci U S A **99**:996-1001.
89. **Steen, E. J., R. Chan, N. Prasad, S. Myers, C. J. Petzold, A. Redding, M. Ouellet, and J. D. Keasling.** 2008. Metabolic engineering of *Saccharomyces cerevisiae* for the production of n-butanol. Microb Cell Fact **7**:36.
 90. **Sugiyama, H.** 1951. Studies on factors affecting the heat resistance of spores of *Clostridium botulinum*. J Bacteriol **62**:81-96.
 91. **Swerdlow, B. M., B. Setlow, and P. Setlow.** 1981. Levels of H⁺ and other monovalent cations in dormant and germinating spores of *Bacillus megaterium*. J Bacteriol **148**:20-29.
 92. **Szulmajster, J., C. Bonamy, and J. Laporte.** 1970. Isolation and properties of a temperature-sensitive sporulation mutant of *Bacillus subtilis*. J Bacteriol **101**:1027-37.
 93. **Tang, H., Y. Mechref, and M. V. Novotny.** 2005. Automated interpretation of MS/MS spectra of oligosaccharides. Bioinformatics **21 Suppl 1**:i431-439.
 94. **Tovar-Rojo, F., M. Chander, B. Setlow, and P. Setlow.** 2002. The products of the *spoVA* operon are involved in dipicolinic acid uptake into developing spores of *Bacillus subtilis*. J Bacteriol **184**:584-7.
 95. **Tsai, M. H., and M. H. Saier, Jr.** 1995. Phylogenetic characterization of the ubiquitous electron transfer flavoprotein families ETF-alpha and ETF-beta. Res Microbiol **146**:397-404.
 96. **Varga, J. J., V. Nguyen, D. K. O'Brien, K. Rodgers, R. A. Walker, and S. B. Melville.** 2006. Type IV pili-dependent gliding motility in the Gram-positive pathogen *Clostridium perfringens* and other *Clostridia*. Mol Microbiol **62**:680-94.
 97. **Walt, A., and M. L. Kahn.** 2002. The *fixA* and *fixB* genes are necessary for anaerobic carnitine reduction in *Escherichia coli*. J Bacteriol **184**:4044-7.
 98. **Warnick, T. A., B. A. Methe, and S. B. Leschine.** 2002. *Clostridium phytofermentans* sp. nov., a cellulolytic mesophile from forest soil. Int J Syst Evol Microbiol **52**:1155-60.
 99. **Warth, A. D., D. F. Ohye, and W. G. Murrell.** 1963. Location and composition of spore mucopeptide in *Bacillus* species. J Cell Biol **16**:593-609.
 100. **Warth, A. D., and J. L. Strominger.** 1972. Structure of the peptidoglycan from spores of *Bacillus subtilis*. Biochemistry **11**:1389-96.
 101. **Warth, A. D., and J. L. Strominger.** 1971. Structure of the peptidoglycan from vegetative cell walls of *Bacillus subtilis*. Biochemistry **10**:4349-58.
 102. **Weiss, K. F., and D. H. Strong.** 1967. Some properties of heat-resistant and heat-sensitive strains of *Clostridium perfringens*. I. Heat resistance and toxigenicity. J Bacteriol **93**:21-6.
 103. **Wen, Q., K. Miyamoto, and B. A. McClane.** 2003. Development of a duplex PCR genotyping assay for distinguishing *Clostridium perfringens* type A isolates carrying chromosomal enterotoxin (*cpe*) genes from those carrying plasmid-borne enterotoxin (*cpe*) genes. J Clin Microbiol **41**:1494-1498.
 104. **Wnek, A. P., R. J. Strouse, and B. A. McClane.** 1985. Production and characterization of monoclonal antibodies against *Clostridium perfringens* type A enterotoxin. Infect Immun **50**:442-448.

105. **Wu, J. J., R. Schuch, and P. J. Piggot.** 1992. Characterization of a *Bacillus subtilis* sporulation operon that includes genes for an RNA polymerase sigma factor and for a putative DD-carboxypeptidase. *J Bacteriol* **174**:4885-92.
106. **Yugari, Y., and C. Gilvarg.** 1965. The condensation step in diaminopimelate synthesis. *J Biol Chem* **240**:4710-6.
107. **Zhao, Y., and S. B. Melville.** 1998. Identification and characterization of sporulation-dependent promoters upstream of the enterotoxin gene (*cpe*) of *Clostridium perfringens*. *J Bacteriol* **180**:136-142.